Doan Alejandro Saavedra Castañeda

Quantitative Seismic Interpretation for the Characterization of Clastic Reservoirs in the Gulf of Mexico

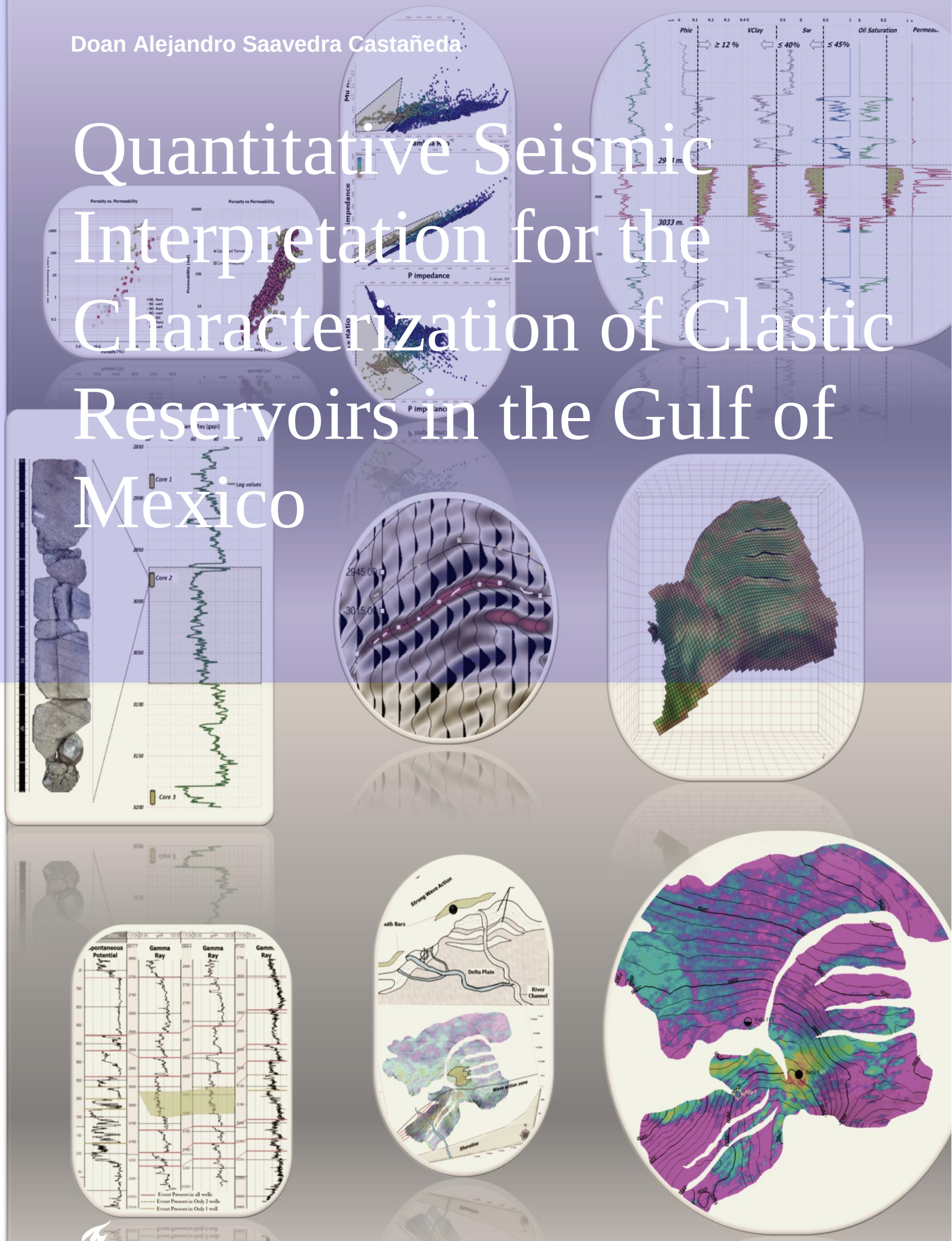

TU Delft

Quantitative Seismic Interpretation for the Characterization of Clastic Reservoirs in the Gulf of Mexico

By

Doan Alejandro Saavedra Castañeda

in partial fulfilment of the requirements for the degree of

Master of Science
in Applied Earth Science

at the Delft University of Technology,
to be defended publicly on Thursday August 18, 2016 at 1:00 PM.

Supervisor:	Dr. J.E.A. Storms	TU Delft
Thesis committee:	Dr. G. Diephuis	TU Delft
	Dr. A. Barnhoorn	TU Delft

Contents

Abstract

New reserves are necessary to compensate the oil depletion of the giant fields in the Gulf of Mexico. This work covers a reservoir characterization workflow of Pliocene shallow marine deltaic sandstone deposits located in the south eastern Gulf Mexico. The traditional reservoir characterization workflow is considered a multidisciplinary integration process in geological and geophysical data is used with the purpose of defining the geometry, internal properties distribution, lateral extension and flow properties of a petroleum reservoir unit. In this study the geological information provided from cores will allow for the understanding of the internal architecture of the reservoir. A petrophysical evaluation was performed in which flow properties such as porosity, permeability, net to gross, and fluid saturations were obtained. Traditional seismic data, has been used for generating a subsurface map of the reservoir units. Sadly, the use of seismic data is subject to a resolution limitation. A novel aspect of the workflow is presented in this thesis: the incorporation of elastic parameters derived from a simultaneous pre stack inversion, which provided the necessary tools to accurately and quantitatively understand the lateral distribution of the reservoir unit. As a result of the reservoir characterization workflow, a reserve estimation was calculated for the newly discovered field. The use of seismic quantitative methods for reservoir characterization helped to correctly delimitate the fluid content and reservoir properties of the field. This will reduce the uncertainty associated with drilling new wells during field development stage.

Acknowledgements

I would like to acknowledge my most infinite gratitude to my wife Ana Garduza, as she is the main reason that kept me going through day and night during my master degree. Without her support I could not have found the strength and the patience to overcome this challenge.

To my beloved family Mrs. Angelica Castañeda for encouraging me and always boosting my mood in times of need, to my father Mr. Domingo Saavedra for showing me the way and teaching me one of the best lessons in life “Hard work, sacrifices and dedications is the key of success”, to my sister Masiel Saavedra for believing in me but above all for inspiring me.

This thesis work was funded by the Mexican Petroleum Oil Company PEMEX, and the National Council of Science and Technology of Mexico CONACYT. Thanks to the support of the CONACYT–SENER HIDROCARBUROS Scholarship, but specially to all the people at CONACYT for the great support and assistance during the duration of my study.

I’m forever indebted to PEMEX for believing in me and allowing me to fulfill a long desired dream, thanks to Mr. Antonio Escalera Alcocer, Mr. Pedro Silva Lopez, Mr. Jose Francisco Gonzalez Pineda, Mr. Guillermo Mora Oropeza, Mr. Jorge Barrios Rivera but specially to my internal supervisor Mr. Damaso Francisco Contreras Tebar for all of his advice and guidance. I would like to also take the opportunity to thank all the help provided by my dear friend Mrs. Mirna Ruiz Lopez.

To my TuDelft supervisors I owe my gratitude: Prof. Joep Storms, Dr. Gerhard Diephuis and Prof. Auke Barnhoorn, thanks for the patience, support, comments and the wisdom that lead to development and improvement on this work.

Lastly I would like to thank all my fellow classmates and colleagues from Delft University of Technology who directly or indirectly help me throughout the duration of my study: Alejandro, Raul, Ricardo, Barnaby, Paul, Duaa, Ellis, Tarek, Martin, Yap, Kai, Febrian, Naveen, Rahul, Robin, Thanasis, Mitra and everyone that helped me survived those long study exam weeks in the library.

1. Introduction

There is great potential for hydrocarbons in Tertiary reservoirs for the Pliocene and Miocene plays located within the Istmo Saline Basin in south-eastern Gulf of Mexico. This area is characterized by high geological complexity, due to salt tectonics which affected the sedimentation in the area. In recent years, various discoveries have been made in the tertiary fields, leading to reserves exceeding 250 MMboe. These recent discoveries have led to the incorporation of new knowledge regarding the geology and petroleum system in this region.

Reservoir characterization generally has two main objectives. The first is to determine the areal delimitation of the reservoir, and the second is to make a realistic estimation of the reserves contained within the reservoir. In order to fully understand these recently discovered fields, I suggest a multidisciplinary geoscience approach formed by geological, geophysical and Petrophysical knowledge with the intent of reduce the uncertainty and quantify different properties present in the reservoir

1.1. Methodology

The main objective of this thesis is to characterize a shallow marine reservoir located within the Istmo Saline Basin in the south-eastern Gulf of Mexico. The traditional reservoir characterization methodology approach will be the basis of this work. In addition, an analysis of a 3D seismic data set and in combination with a facies analysis and petrophysical properties from the different cores and logs present in the area, to determine the internal heterogeneity and map the lateral extension of reservoir.

More specifically, a set of elastic properties volumes will be used to characterize the hydrocarbon fluid associated bodies within the reservoir. The use of the elastic volumes will improve the interpretation and delimitation of the reservoir fluid associated facies.

This thesis work was made possible thanks to the data provided by Petroleos Mexicanos PEMEX. The data set, consist of 4 wells. The name of these wells are Alfa-1, Beta-1, Beta-1St (a sidetrack well of Beta1) and Beta-101. Each of these wells comes with well logging information. A set of three cores from the well Beta-1 will be used to understand the depositional environment of the area.

The core data from Beta-1, comes with a complete Geological report in were the description of the cores are presented. A 3D seismic cube and a set of sub volumes from a pre-stack seismic inversion (p-impedance, s impedance, lambda rho and murho) is also provided. Beta 1 well also comes with a set of well logs curves from a Rock Physic study. These Rock Physics log curves were used as an input, to generate the pre stack seismic inversion.

Based on the provided data, the initial phase of the thesis will consist of evaluation of all the geological data. With the help of the core data, and the geological report, the internal architecture of the reservoir will be studied and a depositional environment will be determined. The second phase of the thesis work consist of analyzing the seismic data.
Synthetics and well-to-seismic matches are created with the purpose of generating a seismic interpretation of the reservoir unit. The seismic interpretation will be accompanied by a structural interpretation phase in were the main faults present on the area will be identified, ending, on a time to depth conversion of the key reservoir level.

The seismic interpretation of the reservoir unit, will be used to generate a set of seismic attributes. These attributes will provide information regarding the distribution of the lithology in the area. Next, a quantitative stage, consisting of the use of the pre-stacked seismic inversion data. Crossplots generated between relevant rock properties and the calculated elastic parameter will help to understand the values associated to the reservoir fluids.

This quantitative analysis will be used to generate quantitative elastic impedance attributes that provide information of fluid distribution at the reservoir unit. Next, once the lateral distribution of the fluids and the lithology are known. A petrophysical evaluation of the reservoir unit will be held. The purpose of this evaluation is to determine the flow associated properties of the reservoir unit. For the final sections of this thesis a volumetric calculation will be performed on the data set. A combination of different seismic attributes will determine the area of the reservoir, while the estimated petrophysical properties will be used as an input to quantify the uncertainty associated to the reserves on the Beta field.

2. Regional Geology

The Beta field forms part of the Southeastern Basins Oil province and is located between the coastal plain of the Gulf of Mexico and the continental Shelf of the southeastern Mexico. The Southeastern Basin area is considered the most prolific area of oil production at national level. In the last 30 years, over 100 wells have been drilled that have led to the discovery, evaluation and production of hydrocarbon reservoirs in the Cretaceous carbonate and Tertiary clastic sediment.

The oil province that is the subject of study in this thesis is formed by the Salina del Istmo Basin, Comalcalco basin, Macuspana basin and the Pilar Reforma Akal basin (Figure 2-1). The Beta field is located in the offshore shallow water area within the Salina del Istmo Basin. This basin is associated with a heavy load of sediment and salt evacuation. The salt present in the area was deposited during the opening of the Gulf of Mexico during the Callovian and early Oxfordian. The diapirism present in the area, initially formed during the compressive stage of the Chiapaneco Orogeny in the late upper Miocene. Finally, during the Pliocene – Pleistocene a change in to an extensional setting, allowed for the development and expansion of the terrigenous sediments deposits filled the basin with mainly shaly succession with some intercalations of sand layers. (Hernández 1973).

The Middle Pliocene Beta field is located in the shallow waters of the Gulf of Mexico, near the states of Veracruz and Tabasco.
The structure of the field can be considered an anticline dome affected by normal faulting in the crest of the structure.

The field has a structural closure in the south against a salt diapir. The reservoir is made of a sequence of sandstones that were deposited on a shallow marine environment. The field was charged by the Thithonian source rock widely spread in the area by a series of migrations paths such the normal faulting present in the area.

Figure 2-1 Location of the Beta Field. The Salina del Istmo Basin is delimited by the purple line.

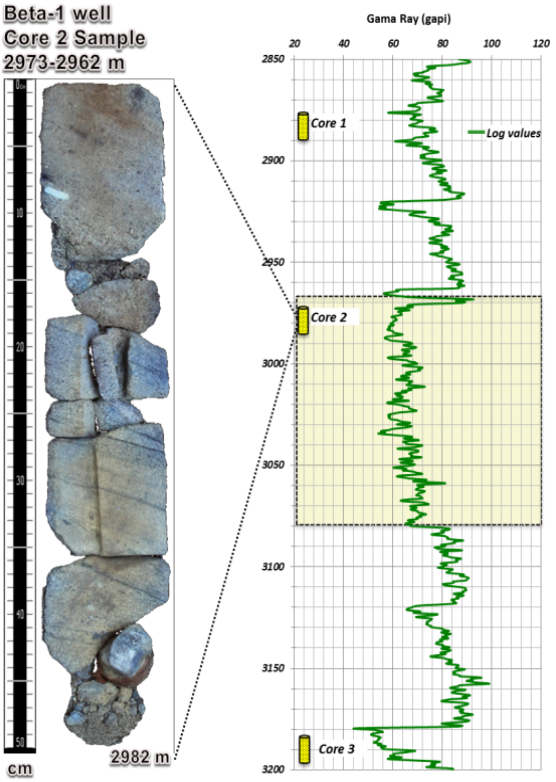

Figure 2-2 Beta-1 well, Main reservoir unit. In this image the position of all the different cores is indicated, as well as the main reservoir unit (depicted in the yellow box).

2.1. Reservoir Unit

Once the regional aspects of field have been described, the next is to describe the generalities of the well that will be used in this thesis work. The newly drilled Beta well will be used as an input to estimate the reserves on the field. Based on the results of the production test the Beta well was classified as an Oil producer with a 33 APIº.

For this thesis work a series of geophysical logs, from the well (Beta-1) and the side track (Beta-1ST) well will be used to understand the properties present in the reservoir. Also with the help of the cores and the Geological report, the internal architecture of the reservoir will be discussed (lithology, porosity, grain size).

The Beta-1 well has three different reservoir units, all of these corresponds to the Lower to Middle Pliocene. The main reservoir unit is show in Figure 2-2, as well as the location of the different core samples.

The main reservoir interval consists of sandstones with grain sizes ranging from middle to fine. The average effective porosity in the cored interval is 18%. Permeability ranges between 100 to 1,000 mD.

3. Internal Characteristics of the Reservoir.

In the following section a brief description of the lithology, grain size, porosity and sedimentary structures is presented. The summary of the most relevant geological features from core 2 corresponding to the main reservoir unit is presented. This summary is based on the geological report provided by PEMEX. Based on the information of the geological report, the depositional environment was re interpreted and compared to the actual geological settings present in the gulf of Mexico.

3.1. Core Description

Core 2 corresponds to the Middle Pliocene and belongs to the depth interval from 2973 m. to 2982 m. This core, is divided into three sections in order to put more detail into it, an upper, middle and lower part. Each of the core sections has been evaluated by a Laser Particle Size Analysis (LPSA), providing information regarding the grain size and grain size distribution. The upper part (2973-2976m) is composed of quartz sandstone deposits. The sample show predominant coarse and very coarse grain to very fine grain size. The grain size distribution and physical structures can be observed in Figure 3-3. The shape of the sand grains is generally sub-rounded to sub-angular and it is poorly sorted. the sample contains At some depth intervals, the presence of calcium carbonate cement is observed. Within the upper section we can observe a fining-up grain size cyclicity at vertical scale of approximately 0.5 m. The base of every cycle represents an erosional surface with the presence of lag deposits (pebbles with a diameter ranging from 1 to 2.5 cm).

One of the main features in the interval is the excellent porosity and the presence of yellow fluorescence due to the hydrocarbons content (e.g. Figure 3-1).

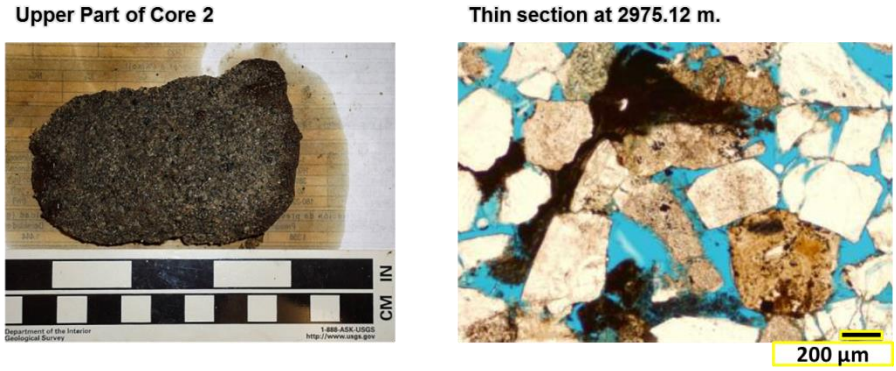

Figure 3-1 Upper part of Core 2. Thin section corresponds to 2975.12. Great intergranular porosity(blue part). The pore space is interconnected. Hydrocarbon presence.

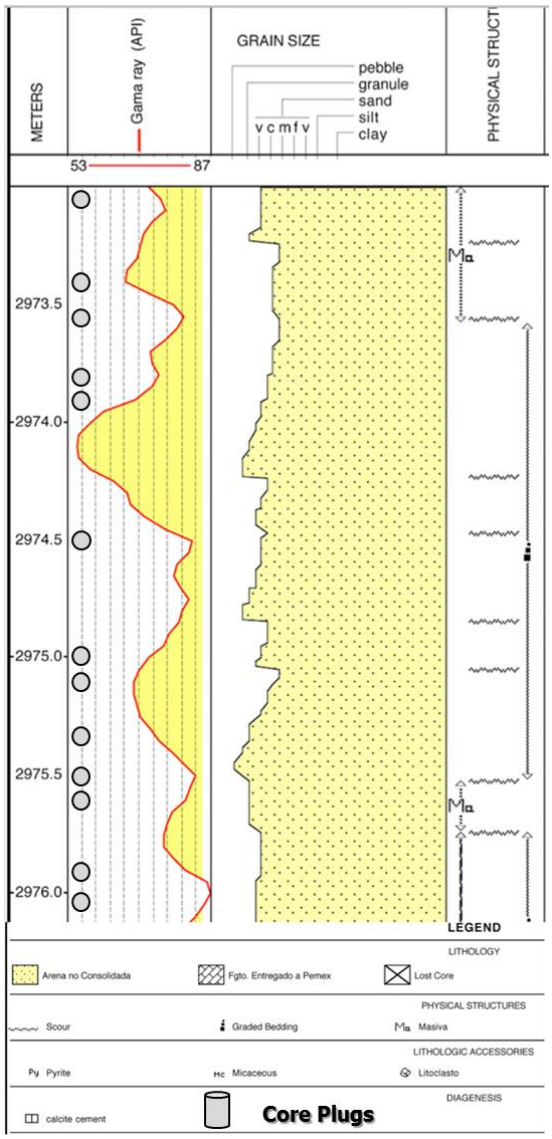

Figure 3-3 Beta-1 Core 2 Upper part description from 2973 m. 2976 m. Grain size distribution and sedimentary structures The grain size distribution was made from direct measurements every 50cm.

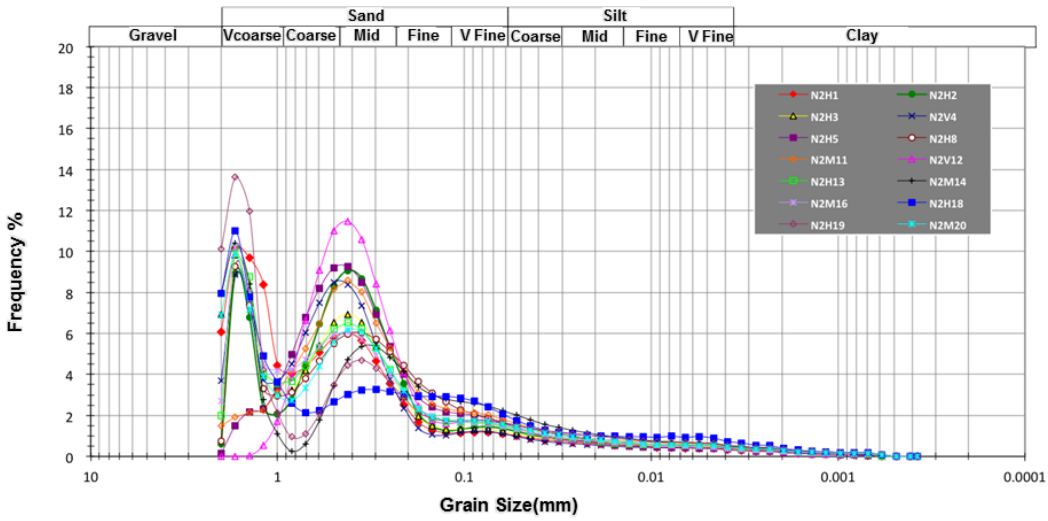

Figure 3-2 Granulometry Analysis samples from (core 2, upper part).

Once the grain size (Figure 3-2) and distribution have been presented, the porosity and permeability of the samples will be discussed. For this core a series of porosity and permeability measurements was performed for a set of core plugs, this core plugs were taken from the previously described core zones(upper mid and bottom). The following table is a summary of the porosities and permeability encountered in the core plugs of this interval.

Table 1 Porosity and Permeability estimation from the upper part of core 2

Sample Number:	N2H1	N2H2	N2H3	N2V4	N2H5	N2H8	N2M11
Depth (meters)	*2973.19*	*2973.42*	*2973.60*	*2973.86*	*2973.91*	*2974.50*	*2975.04*
Porosity (%)	*22.70*	*23.72*	*22.34*	*23.27*	*23.70*	*22.11*	*n/d*
Permeability (mD)	*1948.00*	*2177.00*	*1248.00*	*2681.00*	*2188.00*	*1085.00*	*n/d*
Sample Number:	**N2V12**	**N2H13**	**N2M14**	**N2M16**	**N2H18**	**N2H19**	**N2M20**
Depth (meters)	*2975.12*	*2975.39*	*2975.52*	*2975.66*	*2975.91*	*2976.23*	*2976.41*
Porosity (%)	*23.45*	*23.15*	*n/d*	*n/d*	*24.04*	*24.90*	*n/d*
Permeability (mD)	*1036.41*	*1238.22*	*n/d*	*n/d*	*2043.66*	*1290.94*	*n/d*

The middle part of core 2 is located between 2976 m – 2979m. This interval consist mainly of sandstone. The interval presents very coarse to medium grain size. In different parts of the interval a very fine grain size can be seen. The core samples present a sub-angular shape, it is poorly sorted, and poorly compacted. Throughout the interval sporadic pebbles can be seen, ranging from 1 to 4 cm (Figure 3-4). The sample presents very good to excellent porosity. There is presence of yellow fluorescence due to the hydrocarbons, this can be observed in the thin section from Figure 3-4

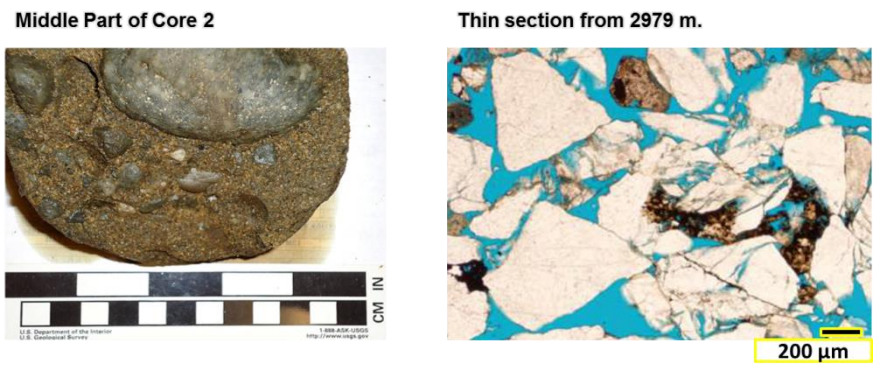

Figure 3-4 Middle part of Core 2. Thin section corresponds to 2979m. the sample has great porosity(blue part). The pore space presents Hydrocarbon presence. Good quality reservoir rock.

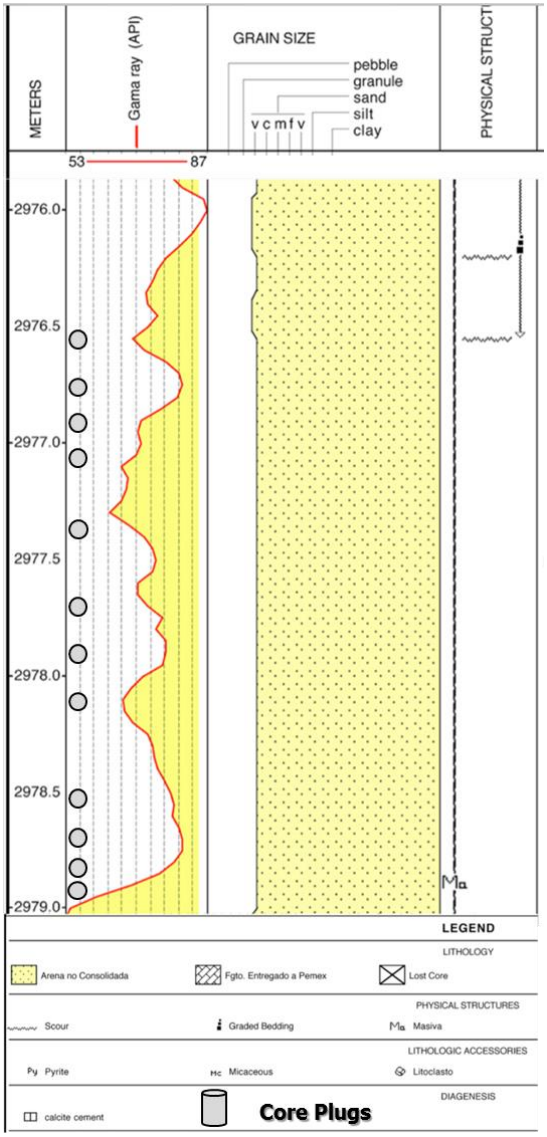

Figure 3-5 Sedimentary structures(scours), gamma ray and Grain size distribution corresponding to the Core 2 Middle part.

Table 2 Porosity and Permeability obtained from the core plugs of the mid section.

Sample Number:	N2H21	N2H22	N2H23	N2M24	N2M25	N2M27	N2M28
Depth (meters)	*2976.56*	*2976.68*	*2976.88*	*2977.29*	*2977.43*	*2977.71*	*2977.94*
Porosity (%)	*26.03*	*23.53*	*23.69*	*n/d*	*n/d*	*n/d*	*n/d*
Permeability (mD)	*2662.48*	*2005.91*	*2245.86*	*n/d*	*n/d*	*n/d*	*n/d*
Sample Number:	**N2M30**	**N2M32**	**N2H33**	**N2H34**	**N2H35**	**N2M36**	**N2M38**
Depth (meters)	*2978.26*	*2978.52*	*2978.70*	*2978.82*	*2978.93*	*2979.29*	*2979.51*
Porosity (%)	*n/d*	*n/d*	*24.98*	*23.75*	*25.93*	*n/d*	*n/d*
Permeability (mD)	*n/d*	*n/d*	*2366.97*	*2388.40*	*2550.41*	*n/d*	*n/d*

The gamma ray from the middle part of the core is presented in Figure 3-5. The value of the gamma ray corresponds to a sandstone. This interval exhibits 2 scours structures throughout the interval. This figure also shows that the overall grain size corresponds to coarse sand in the sample, in were the dominant grain size is medium coarse. The porosity and permeability estimated from the core sample is shown in table 2.

The lower section of the Core 2 (from 2979 m. - 2982 m) is mainly composed of quartz sandstone (Figure 3-6) The samples display a predominant presence of very coarse grain to very fine grain with sub-angular to sub-rounded grain shape. The sample is poorly sorted and cemented by calcium carbonate. This interval shows an abundant presence of pebbles with a diameter ranging from .5 to 2.5 cm.

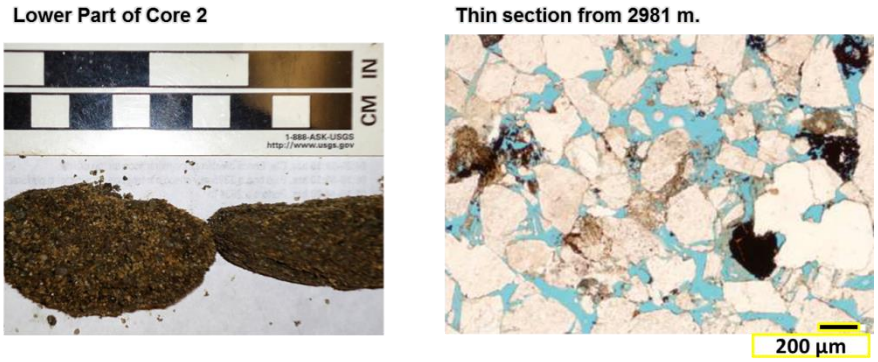

Figure 3-6 Lower section of Core 2. Poorly consolidated sandstone, with good porosity and hydrocarbon content.

As shown on the right side of Figure 3-6, the sample presents good porosity, this is visible in the thin section. Also the presence of hydrocarbons is evident. The next table is the summary of the porosity and permeability obtained from the special core analysis. The overall porosity and permeability values from core 2 can be considered as a reservoir unit with an average porosity of 22% with an excellent permeability.

Table. 3 Data obtained from the 14 samples of the core plug, (core 2, lower part).

Sample Number:	N2M39	N2M41	N2M42	N2M44	N2M45	N2M47
Depth (meters)	*2979.70*	*2979.94*	*2980.04*	*2980.24*	*2980.51*	*2980.73*
Porosity (%)	*n/d*	*n/d*	*n/d*	*n/d*	*n/d*	*n/d*
Permeability (mD)	*n/d*	*n/d*	*n/d*	*n/d*	*n/d*	*n/d*
Sample Number:	**N2M49**	**N2M50**	**N2M52**	**N2V53**	**N2M54**	**N2H55**
Depth (meters)	*2980.96*	*2981.20*	*2981.44*	*2981.71*	*2981.88*	*2981.95*
Porosity (%)	*n/d*	*n/d*	*n/d*	*25.19*	*n/d*	*23.51*
Permeability (mD)	*n/d*	*n/d*	*n/d*	*2449.61*	*n/d*	*2956.19*

To summarize the 3 sections of the core present good porosity and hydrocarbon content. This specific components is the basics for considering a good reservoir rock. In spite of this, the 3 core samples have differences between them. The upper part of the core is characterized by having a graded bedding behavior and it shows the presence scours. The middle part is characterized by having a predominant coarse grain size. Finally the lower part of the core shows the presence of pebbles ranging in diameter from .5 to 2.5 cm. Overall the geological feature present in this core samples, provide a useful information regarding the reservoir units basic characteristics.

4. Depositional Environment

After a brief geological description of the reservoir unit, the depositional environment will be discussed in the following section. The information presented in this chapter is the result of the examination of the geological report from Pemex and based on information encountered during this work. The depositional environment is one of the key factors in understanding the geological conditions in which the sediments were deposited. A sedimentological analysis provides geological clues about the way the sediments where transported. This also provide clues regarding the distance that the sediment traveled. Finally, based on this evidence, it is easier to understand in what kind of geological environment where the samples deposited.

The different sedimentary structures, encountered in the core analysis are shown in Table. 4-1. These sedimentary structures provide information that can be used to better understand different sedimentary facies. The term of sedimentary facies can be defined as a series of similar geological characteristics present in different samples. These similar characteristics shared between samples can vary from sedimentary structures to grain sizes or color.

Table. 4-1 Sedimentary structures present on the core data

Sedimentary Structures	***Core 1***	***Core 2***	***Core 3***
Load Cast			x
Hummocky Structures			x
Cross Stratification	x		
Planar Lamination	x		
Scours		x	x
Erosional Surface			
Bioturbation	x	x	

In general, the facies identification is a process where the sample presents characteristics that are exclusive to a particular geological environment. The combination of the sedimentary structures, paleontology, and the paleobathymetry information from the geological report, will provider answer regarding the depositional system.

The samples correspond to a shallow marine environment. This was deduced from the paleobathymetry report provided by PEMEX. This data provides the most reliable information regarding the water depth of the system during the deposition of the samples as it uses the micro paleontological present in the samples. Base on the benthic foraminifera encountered in the data (Lenticulina americana, Quinqueloculina lamarckiana) the water depth was determined. With this information, the selection of the different possible geological scenarios environments is narrowed down.

One of the sedimentary structures interpreted form the cores, shown on Table 5-1, is specific to a depositional environment, such as hummocky cross stratification. These kind of structures are exclusively the result of storm influenced environments (Dott & Bourgeois 1982). One of the characteristics of the Hummocky cross stratification structures is that these structures are normally only seen in fine to medium grained sand, suggesting that there is some grain size limitation involved in this process. (Nichols 2009).

According to the interpretation of the geological data, presented on the geological report the depositional environment of the reservoir unit corresponds to a series of sand bars deposited over a shallow marine platform, the associated facies is considered a set of sand bars and channels deposited during the early Pliocene. This interpretation did not provide more detail since the study area is widely known due the number of wells drilled in the area.

Here we will reinterpret the data to specify the paleo depositional environment. The deposits and sedimentary structures from the core 2 shows no evidence of tidally influences deposits. The core description mentions the presence of Hummocky cross stratification structures (Figure 12-1). Although identifying these structures is complicated in a core, they provide a clue regarding the depositional environment.

The presence of these sedimentary structures, indicate that we are dealing with sediments that were deposited on on a wave-influenced enviroment. Based on this the depositional environment is reinterpreted as a wave dominated delta. Wave dominated deltas (Figure 4-1) are associated with strong winds that rework and redistribute sediments deposited in shallow water.

,

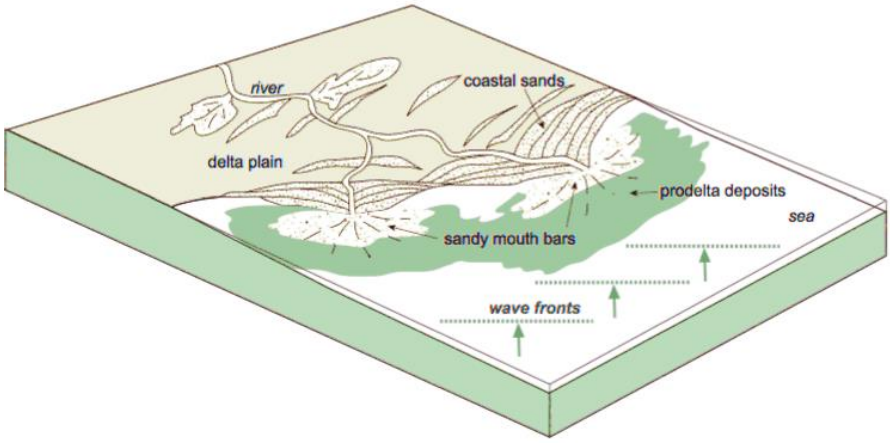

Figure 4-1 Conceptual model of a Wave dominated delta. (taken from Nichols 2009)

This wave dominated delta can be considered a modification of a traditional river or delta environment. The main difference is that the wave actions redistribute the sediments, generating sedimentary structures. The progradation of the distributary channel towards the ocean is limited because of the waves action due to a wave – induced litoral drift of sediment. This propitiate a lateral migration of sediment as the waves wash material along the coast to form beach deposits and mouth bars that build up as elongate bodies parallel to the coastline (Flemings 1995).

In order to fully understand if the geological features present in the core description provide an accurate description of the depositional environment, the wells present in the area where analyzed.

5. Well Correlation

The cored interval of Beta-1 well corresponding to the reservoir unit (figure 3-1) has been interpreted as part of a wave-dominated delta in the previous chapter. At this cored interval the section consists of <0.5 m event beds with a typical fining up succession. However, at a larger scale (2967-3080m depth). The core 2 represents only the upper part of a thick coarsening upward succession which represents the reservoir unit. This thick Coarsening Upward succession lacks clear marine flooding surfaces. The lateral extent of this parasequence can be determined by correlating the nearby wells which is important to correctly understand the lateral extent of the reservoir unit.

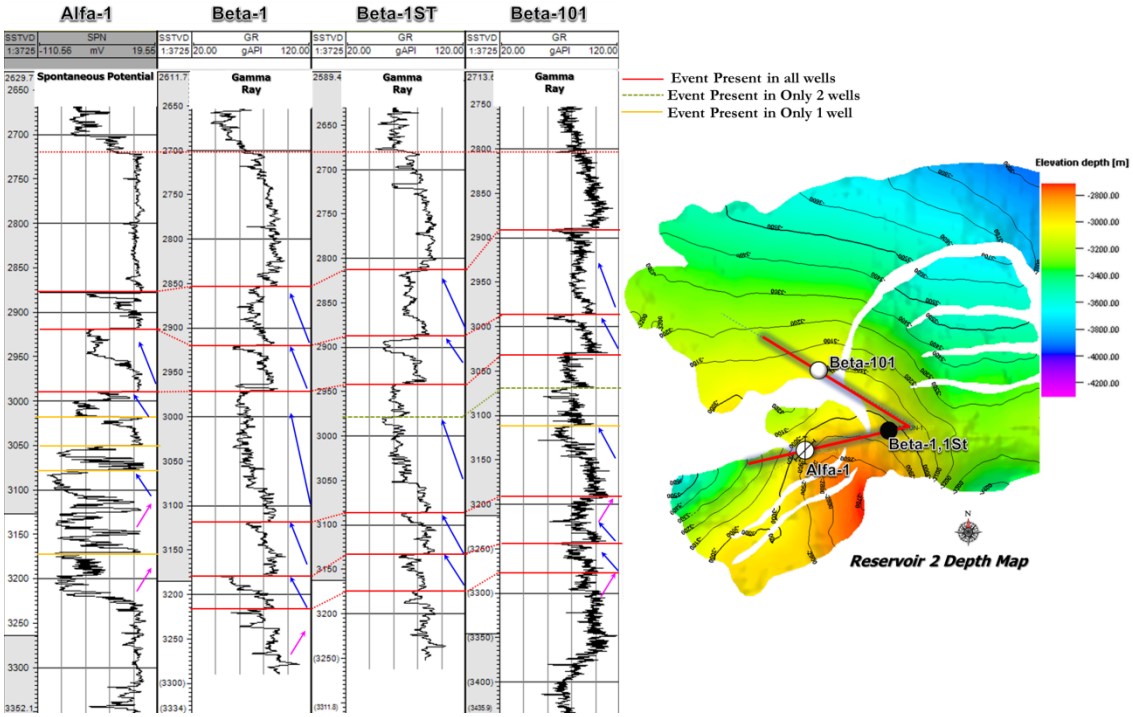

Figure 5-1 Geological Cross section between the wells present in the study area. The blue arrows showing a transition from shale to clean sand, while the pink arrows show the opposite transition from clean sand to shale. On the right of the image, the reservoir unit

Figure 5-1 shows a cross section of the wells that have been flattened to a consistent and regional reservoir seal. It can be seen that multiple parasequences can be identifies in wells Beta-1, Beta-1st and Beta-101 and that they align between the wells.

From Figure 5-1 it is evident that all of the wells display differences in the gamma ray behavior. Starting from the Alpha -1 well, the spiky gamma ray behavior of this well corresponds to a more channelized nature. As Alpha-1 consists of predominantly channel deposits alternated by floodplain fines, it is not possible to correlate the reservoir unit in wells Beta-1 and Beta-101 to Alpha-1. The connectivity between the Beta well and the Alpha well is therefore not clear. Based on the the gamma ray behavior on the Alpha well, it suggests a sediment point sources related to a river.

On the contrary, the Gamma Ray response of the Beta-1 and Beta-1st wells consists of approximately the same unit thickness, as well Beta-1st is a deviated well from Beta-1, the gamma ray responses of these two wells are almost identical. Regarding the Beta-101 well, three coarsening upward successions at the reservoir interval can be identified. This succession's merge into one thick amalgamated sand succession in Well Beta-1.

Once the lateral extent of the reservoir unit is known, as a final step on understanding the depositional environment the present geological conditions will be analyzed. Based on the work done by Padilla 2014 the paleo coastline is likely to have an overall similar orientation as the present-day coastline. The present day geology conditions can be considered similar to the deposition time. Figure 5-2 shows the actual conditions in the Gulf of Mexico, described above in the Depositional Environment section. The Mexican National Institute of Geography (INEGI) reports strong erosion in the area, this erosion is represented by the white arrows colliding against the actual coast line. The driving force is the wave action. The current depositional environment, close to the Grijalva delta is shown in this Figure. It is evident how the wave action generates erosion on the previously deposited sediments of the Grijalva River. The actual conditions of the Gulf of Mexico, also support the theory of the wave dominated delta.

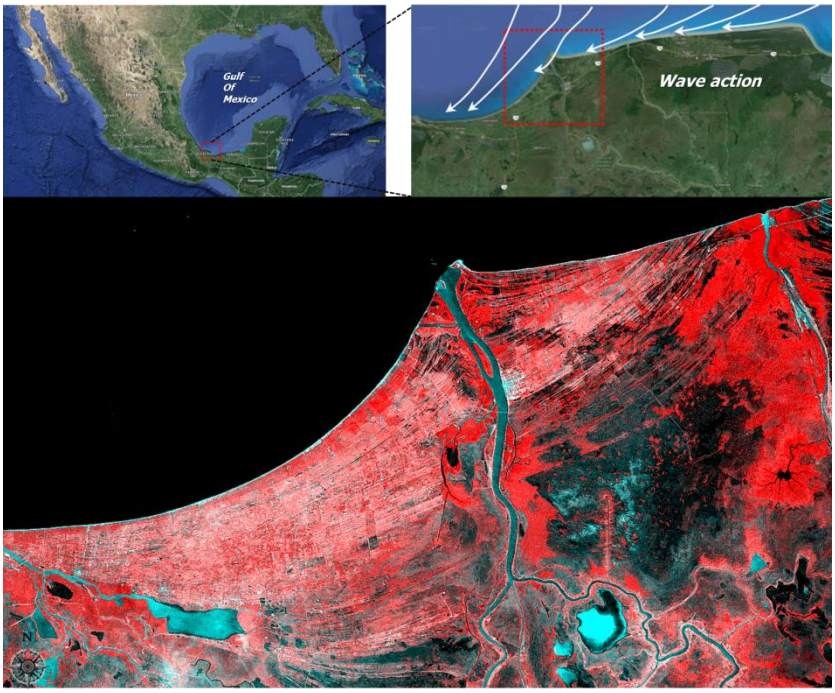

Figure 5-2 Satellite image providing information regarding the actual geological depositional environment (Google maps 2016)and (INEGI)Strong wave action in the Grijalva River area, shown in the picture by the white arrows eroding the coast line.

The Figure 5-3 can be used as a summary of the described in the Depositional Enviroment chapter. This figure represents a geological 2D depositional enviroment based on the evidence provided from the core analysis and the present day conditions od the Gulf of Mexico. This image can be used to understand the different gamma ray trends present in the different logs. As mentioned the Alfa well shows a more chanalized behavior. This behavior can be explained in the 2D model and also in the satelite image of the Grijalva river (Figure 5-2). The main channel of the Grijalva river has migrated laterally over time within the chanel belt. This behavior may explain the spiky behavior of the log. Since the coastile have a coinciding aperance as the present day settings, it can be inferred that Beta1-1 is likely to be located in paleo seaward from Beta-1.

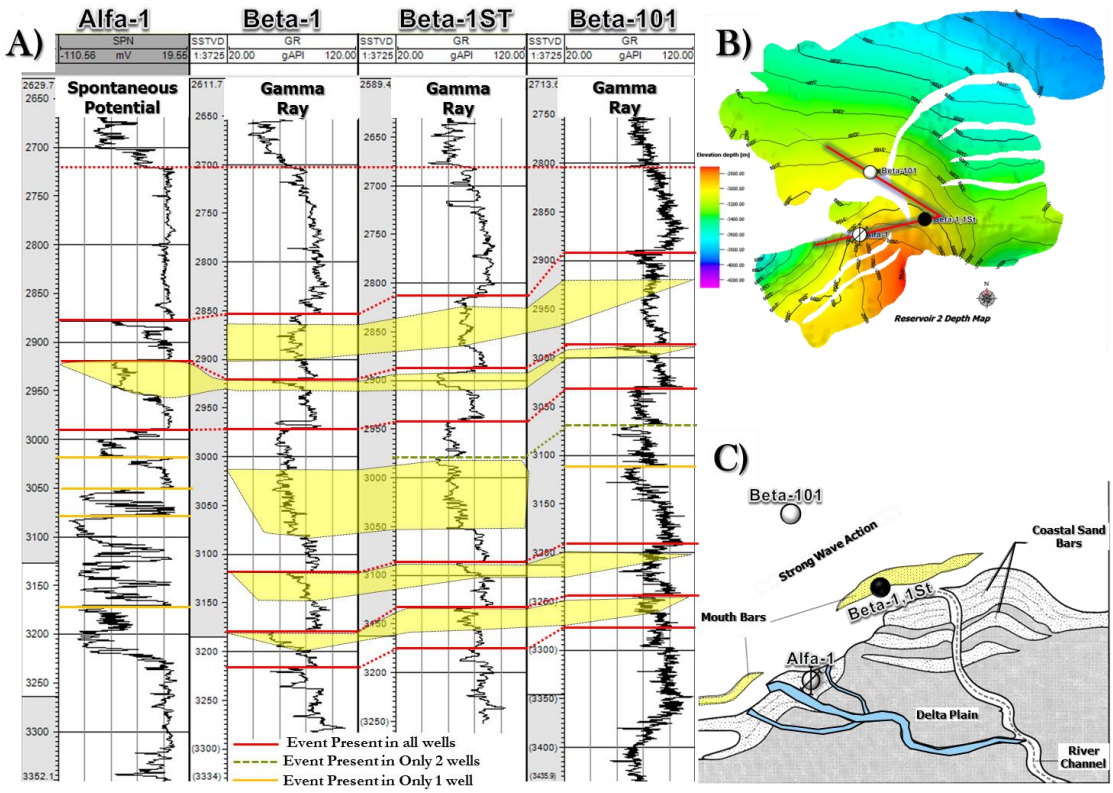

Figure 5-3 A) Geological Cross section of the wells present in the area. B) the direction of the geological over the reservoir unit map. C)2D depositional environment is proposed as a waved dominated delta based on the trends of the Gamma Ray.

6. Seismic Data

6.1. Introduction

3D seismic data have been used in the oil and gas industry for more than 60 years, starting on the beginning of the 50's. The seismic data has not only been used to generate a subsurface maps but more recently to infer reservoir properties from the analysis of the seismic amplitudes from different set of attributes

6.2. Generalities of the Seismic Data

The seismic data set used in this thesis work belongs to series of marine acquisitions volumes from the south east of the Gulf of Mexico. The total area of the original survey is 5000 km^2. This thesis will focus on the area around the "Beta" field, this sub volume consists of 100 km^2 (Figure 6-1). The range of inlines varies from 1530 – 4480 and the range of xlines has a range from 11241 to 14712, this sub volume has a bin size of 25m by 25 m. More detail regarding the acquisition parameters of the data set can be seen in the Appendix.

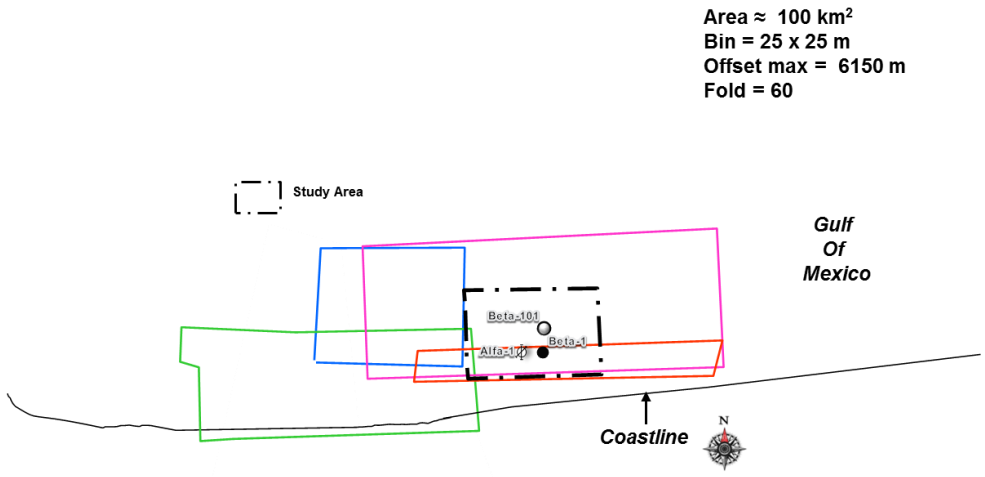

Figure 6-1 Seismic survey location and specifications

6.3. Seismic Resolution

In order to calculate the seismic temporal resolution over the Reservoir level (Figure 6-2), a 200 ms time window was selected to perform the analysis. The first step is to calculate the dominant frequency over that time window, in this case a frequency of 20 Hz was determined for the selected interval. The resolution is determined by taking into account the half a dominant wavelength followings the Rayleighs criterion, in this case a 25 ms was estimated.
Once the temporal resolution is known, the calculated interval velocity of 3100 m/s was used to obtain a 39 meter resolution in depth.

$$f = \frac{\#\ cycles}{Time\ window} = \frac{4}{200\ ms} = 20\ Hz.$$

$$b = \frac{1}{f} = \frac{1}{20} = .05\ \ and\ \frac{b}{2} = 25\ ms$$

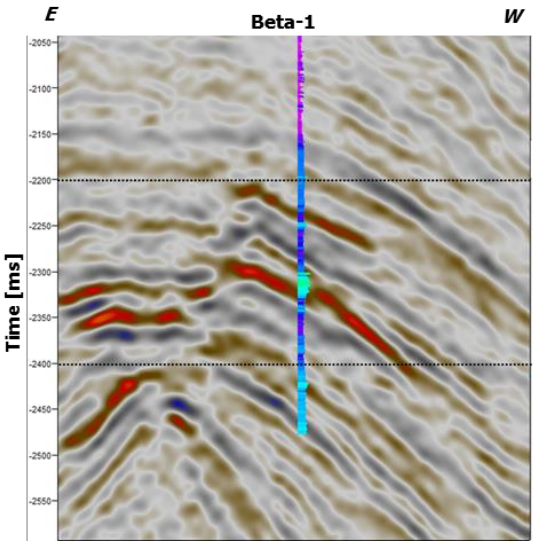

Figure 6-2 Seismic section of well Beta-1, reservoir level.

6.4. Well to Seismic Match

The importance of the synthetics is to derive the acoustic response in terms of Reflection coefficient. This unique response corresponds to a specific geological unit, in which the geological features such as density porosity and fluid content of the rock generate an hard or soft kick.

In order to generate a synthetic seismogram, it's important to understand the shape of the seismic signal, and also to understand the geological response shown on the calculated reflection coefficient series. From this process there are several outputs that are of great importance to the interpreter, such as understanding the phase and polarity of the data set, identifying main geological boundaries.

The way the synthetic is calculated is by first generating the Acoustic impedance, this is realized by multiplying the sonic log with the density log, it is important to mention, that this logs where complete on the reservoir level, there was no need to calculate missing values. The resulting acoustic impedance is used to generate a series of reflection coefficients at each interface between the contrasting formations. Once the reflection coefficients a wavelet is extracted from the traces near the well position, and this wavelet convolved with the reflection coefficients generating a synthetic seismic trace. The process end with the conversion from depth to time. Once the synthetic is made, it is easy to find the correct correlation of the geological markers, based on their specific characteristics to the seismic events.

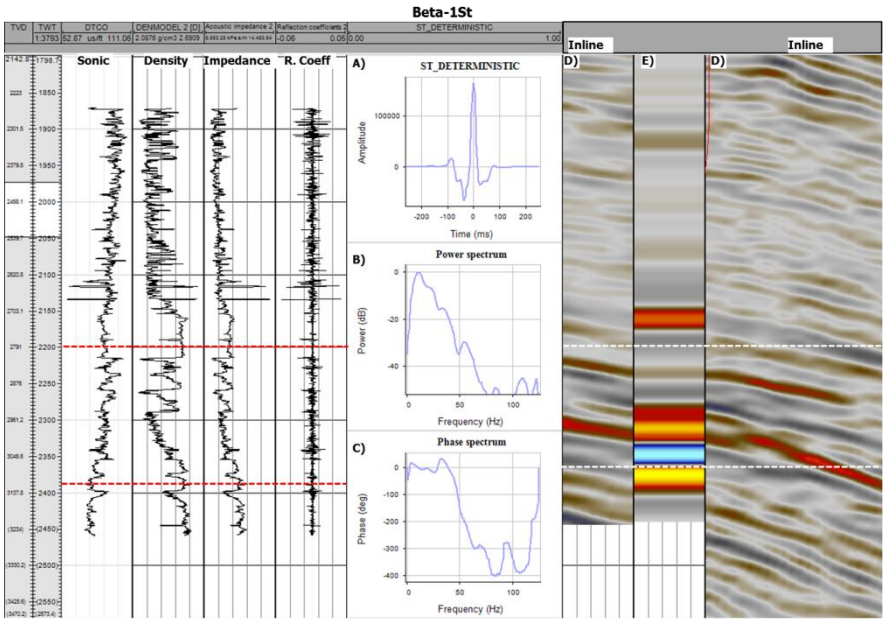

Figure 6-3 Synthetic seismogram calculations showing the basic logs used to calculate the Acoustic impedance and Reflection coefficients., A)wavelet extracted from the well Beta-1st,.B)Frequency content., C) Phase spectrum of the wavelet, showing a zero phase behavior., D)Inline of the Seismic Data set being compared to the Synthetic seismogram shown in E).

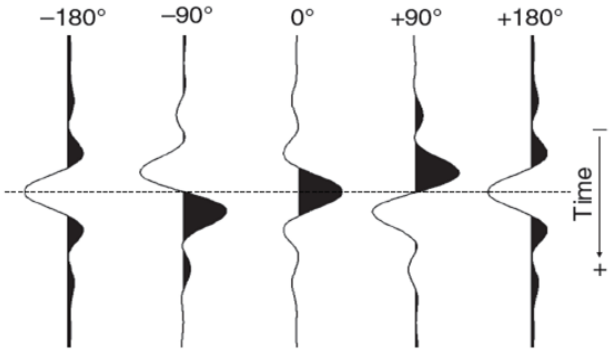

Figure 6-4 Phase rotation of a zero phase wavelet.

One of the key aspect of the seismic interpretation process in which the objective is to use the seismic amplitudes to generate a map of the subsurface, is the shape of the wavelet. From the interpreter's point of view the ideal wavelet is a zero phase wavelet, this is shown on the center of the Figure 6-4. This is considered the best wavelet because it presents unique features such as having a symmetrical shape and most importantly it has the amplitude centered on time zero, this peak amplitude is representative of the causal reflection coefficient.

As previously mentioned the zero phase wavelet is ideal for the seismic interpretation process, this is mainly because its central peak at zero time. This represents an interface change between layers of different impedance values, this change impedance contrast will be correctly represented by trough or peak. This makes it fairly easy to relate the seismic trace to the subsurface layering. (Brown 2011).

From the well tie produced from well Beta-1St (Figure 6-3) the interest zone is delimited between the red lines on the logs and the white lines on the seismic data, this reservoir levels are considered low impedance reservoirs, this behaviour is more easily shown on (Figure 6-5). The extracted wavelet using the White method (White 1997), is consider to be a zero phase wavelet, and the seismic bandwidth is estimated to be ranging from 8 to 40 Hz.

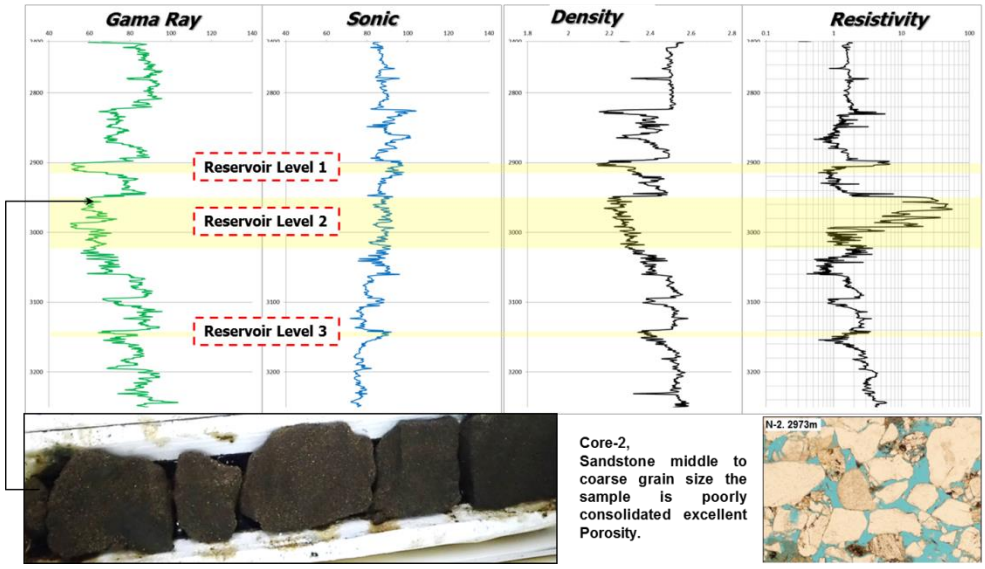

Figure 6-5 Beta-1St logs, showing the response of the 3 reservoir levels shown in yellow, this 3 intervals show low impedance behavior, based on a clean gamma ray values and the low density and low sonic values.

After reviewing main features from the Seismic data previously described in this chapter, and based on the information provided by the SEGY header and from the wavelet behavior. A series of issues resulted from the extraction of the final wavelet, this will be discussed next. The information provided by the SEGY header, mentions that the standard SEG format is used in all of the processing sequences, this means that the acquisition polarity was maintained throughout processing stage and it also refers that the storage polarity has been respected.

The recommendation of a SEG committee on polarity published by Thigpen et al. (1975). Mentions that an increase in pressure on a hydrophone should be recorded as a negative number and displayed as a trough. This means that a transition from a soft event into a hard event (hard reflection) will be recorded as trough. This is represented on Figure 6-6. This recorded hard reflection, later after the processing and following the standard SEG American Polarity will be visually displayed as a central peak in the positive event, it is important to mention that the used data is considered American Polarity.

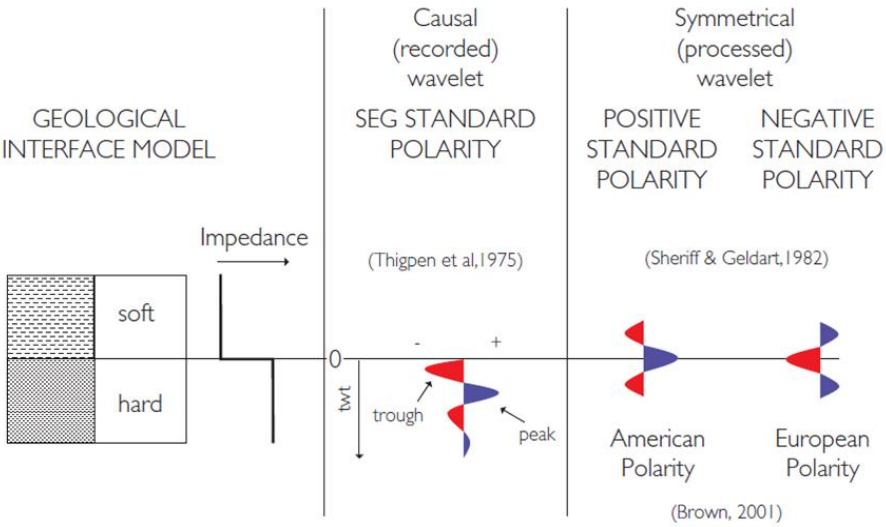

Figure 6-6 Seismic polarity conventions, Image taken from (Simms & Bacon 2014)

It is know that in the Gulf of Mexico the expected reflection coefficient for salt bodies traditionally to be a hard kick for the top of the salt. So in order to be certain regarding the Polarity of the data set, a series of known reflection coefficient were analyzed, in this case the sea bottom (positive reflection) and salt bodies (positive reflection) both of them shown signs of the expected hard kicks.

The encountered problem with the extracted wavelets can be observed from the behavior shown on the synthetic (Figure 6-3 A), as the wavelet was extracted from the reservoir unit. The reservoir it is known to be a low impedance reservoir. This reservoir unit is displayed in the seismic as a negative reflection coefficient (troughs). The main problems comes from the extracted wavelet, as the central peak is centered as a positive number and thus if this wavelet is convolve with a positive reflection coefficient it will generate a positive number. This behavior is a clear indicator of a polarity change to the data set. Despite this discovery, the interpretation stage won't be affected by this, since the synthetic correctly shows that the seismic data is correctly visually displayed.

Once all the interesting geological events were identified in the log data and correctly matched with the seismic data, the next step is to realize the geological interpretation of the desired intervals, in this case the reservoir levels.

6.5. Interpretation of Horizons

Based on the information generated from the well to seismic matching, and knowing that our data sets behaves as a zero phase wavelet, the seismic interpretation process can start. The Beta-1St, presents 3 reservoir zones, shown on (Figure 6-5 Yellow zones.), the seismic interpretation process started, generating a cross section between the wells in the area, in order to correctly identified the correct seismic event, preventing errors on the interpretation process. The interpretation process was realized every 10 Inlines and Cross lines, and in zones with geological complex structural behavior, the grid was reduced to a 5 by 5 spacing grid. On the following images the interpreted horizons can be displayed (Figure 6-7).

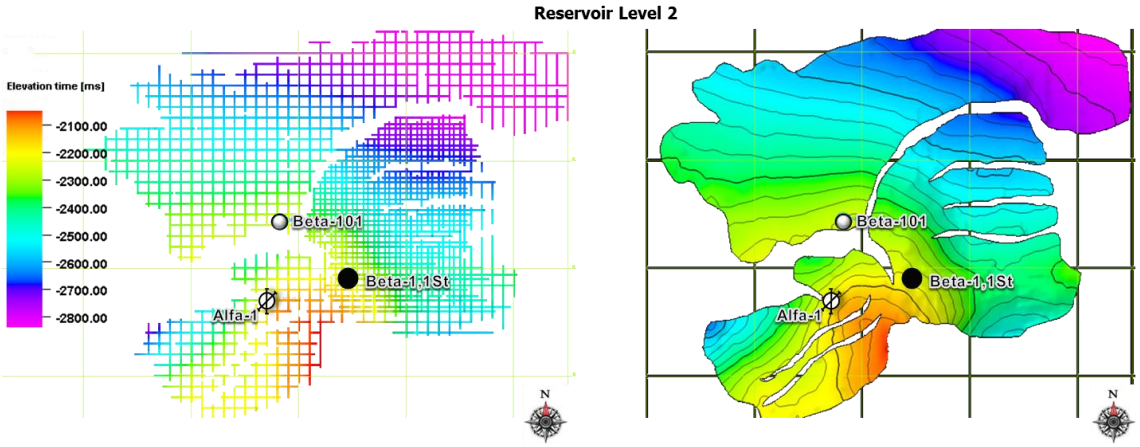

Figure 6-7 Reservoir level 2, Interpretation grid left picture, Final surface in time right picture.

6.6. Depth Conversion

After the seismic interpretation process has ended, and the different maps of the reservoir levels were generated by a manual interpretation pick on the seismic volumes in time domain, the next step is to accurately create a true representation of this time structures in the depth domain, once this time maps are on the correct domain. This will be the input need it to build an accurate reservoir model in where the volumetric can be calculated.

This mapped time structures (Figure 6-7) need to be converted into depth, always taking into account that there must be a correct correlation between the well markers and the new depth maps. The methodology used to do the depth conversion was the Layer cake velocity model, it is important to mention that this methodology provide an accurate result in the well locations, and as we move away from this point the accuracy decreases.

Using the Interval velocities is the key to find the accurate and representative velocity that corresponds to a specific geological layer, the following equations was used to correctly estimate the Interval velocities of the reservoir level. The final calculation of the Interval velocities used for the layer cake velocity model is shown in Appendix (Table1and 2)

$$V_{int} = 2 * \frac{\Delta Z}{\Delta TWT}$$

Once these calculations were realized, it was estimated that for the Reservoir level an Interval velocity of 3200 ms was calculated. It is important to mention that interval velocities get progressively worse for greater depths and also for thinner beds. The final depth surfaces are shown on (Figure 6-8) after the depth conversion process. These depth structures will be the input for the following steps. This is why this process is so important and should be as accurate as possible.

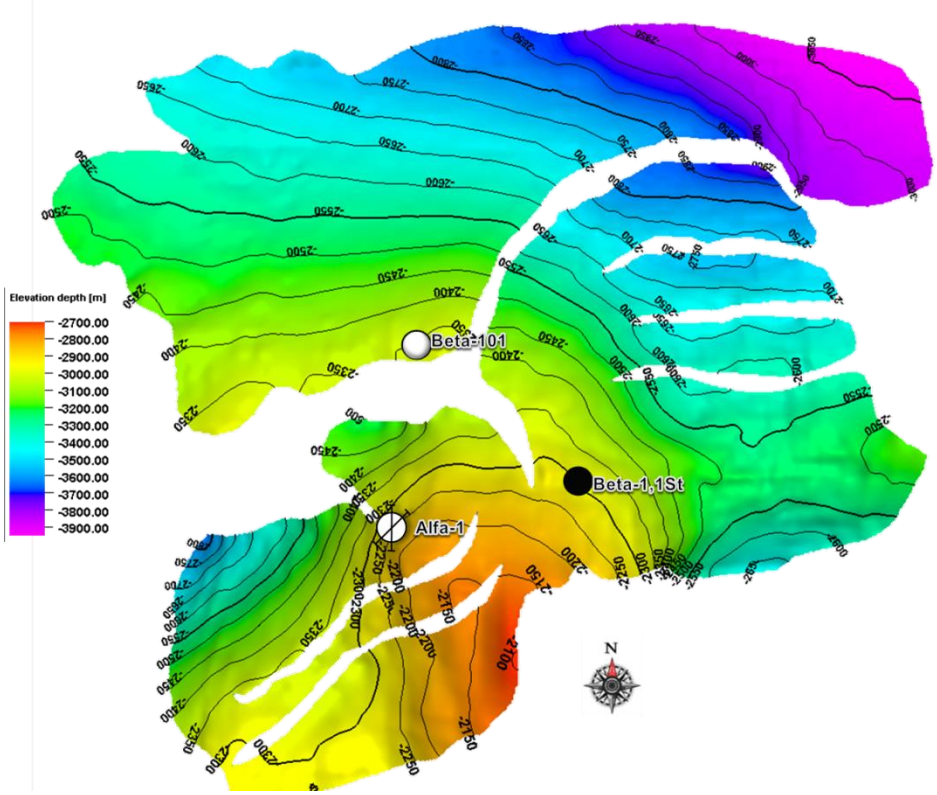

Figure 6-8Final Depth converted map.

6.7. Forward Modeling

A key concept in interpreting seismic amplitudes is an understanding of how rock properties are affected and modified by a change in fluid in fill; for example, by changing the reservoir zone from Hydrocarbons to brine. This process will provide the necessary information on what to look for and what to expect from seismic amplitude responses in specific geological settings. This will be realized by the creation of synthetic logs for a different set of fluid scenarios based on the available well log data.

The selected method to realize this forward modelling is the fluid substitution Gassmann's methodology. In general, this method provides information about the effect of replacing brine with hydrocarbon on a reservoir interval, this will generate a change in the P wave velocity and the density of the rock. The Gassmann's equation shown next, describes the rock in terms of the bulk moduli of a two phase medium (fluid content and the matrix)

$$k_{dry} = \frac{k_{sat,1} \cdot (1-\phi) + k_{sat,1} \cdot \frac{k_S}{k_{fl,1}} \cdot \phi - k_s}{\frac{k_{sat,1}}{k_s} + \frac{k_s}{k_{fl,1}} \cdot \phi - (1+\phi)}$$

K_{sat} bulk modulus of the fluid saturated rock.
K_0 bulk modulus of the matrix material.
K_d bulk modulus of the dry rock frame.
K_{fl} bulk modulus of the pore fluid.
μ_{sat} shear modulus of the fluid saturated rock.
μ_d shear modulus of the dry rock frame.

Two scenarios were calculated and presented on Figure 6-9. The first scenario consist of a 100% of oil saturation, and the second one is a scenario in which the assumption of a 100% water saturation was modeled. This two scenarios are compared with the in situ fluid content, and it is easy to see how the Sonic velocities are affected when introducing hydrocarbon in to the system, the P velocities decreases.

However, the contrary occurs when the 100% water saturation in where the P velocities increases. It is important to mention that shear modulus is not affected by pore fill, effectively because shear waves do not travel through fluids.

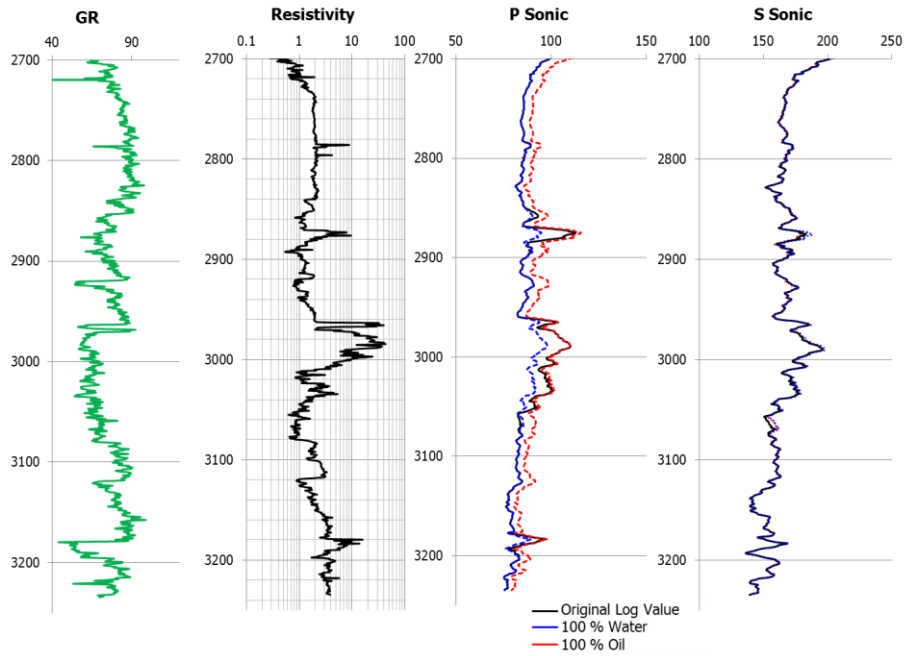

Figure 6-9 Fluid substitution done to the Beta-1St, in black the insitu fluid content, red a scenario with a 100% Oil content, in blue a scenario where a 100% water saturation.

The fluid substitution was realized on the entire log set, but the specific parameters for the equation were taken from the reservoir levels. Figure 6-10 shows how this fluid substitution affects the P and S velocities. The reservoir intervals are shown with in the yellow boxes, the response of the P velocities on the reservoir level provides information on how, by incorporating hydrocarbons to the pore system, generates an decrease on velocities.

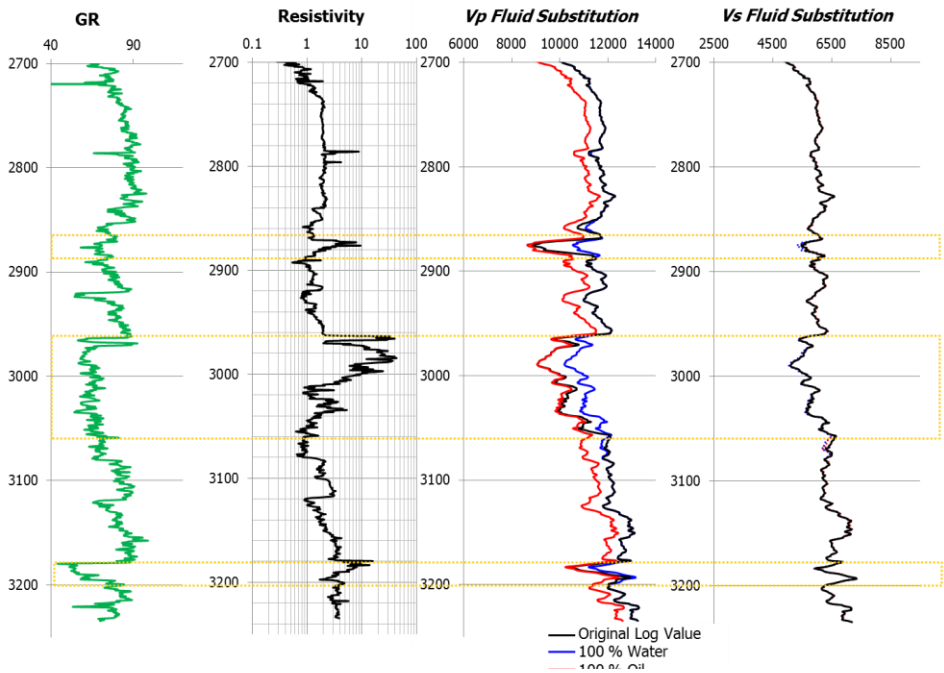

Figure 6-10 Fluid Substitution. Vp and Vs responses are shown, by changing the in situ fluid properties.

Finally, once the different set of velocities where calculated, on (Figure 6-11) the vp vs ratio is presented. After this fluid substitution was realized, it is easy to understand that the reservoir level is considered a low impedance reservoir.

Based on the calculated, fluid sustitution on the reservoir. It generates a change on the velocitites and densities, this can be used as an indication of posible changes in the impedance behavior. This can be used to find a possible oil water contact, in which the initial low impedance reservoir, when facing a fluid substitution to a 100% water saturation, presents a change in impedance behavior generating a possible change in the seismic volumes, from a soft kick to a hard kick.

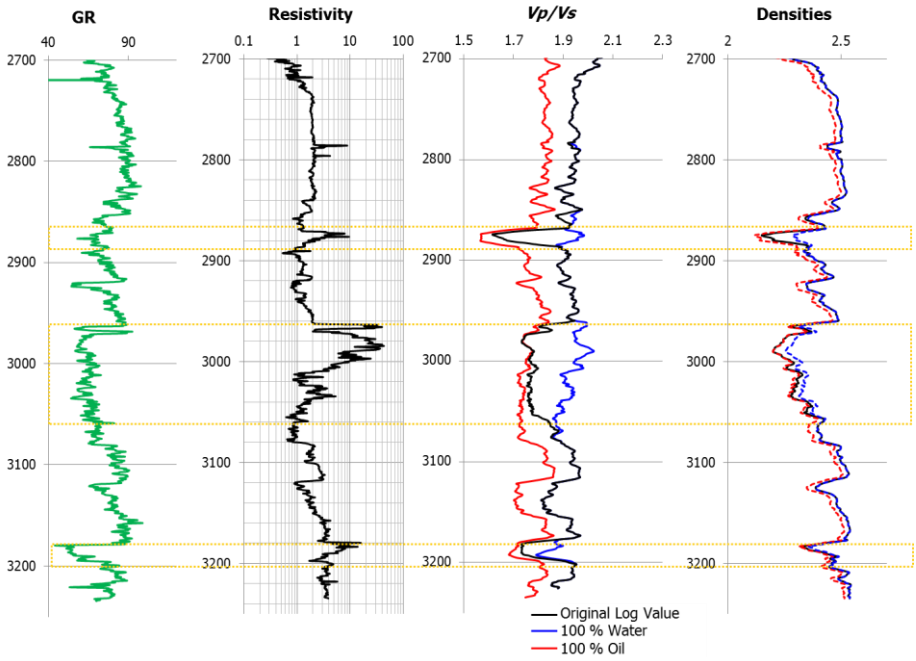

Figure 6-11 Fluid substitution set, Vp/Vs ratio is shown.

The OWC (oil water contact) was detected based on the results from the MDT test (Modular Formation Dynamics Tester) presented on (Figure 6-12). All of the samples taken from the MDT analysis are plotted in the right side of the image. Pressures and fluid samples were taken from the reservoir interval.

The OWC can be detected by a change in the pressure gradient from hydrocarbon samples (Red points with green values). Based on this MDT test, a change in pressure gradient occurs at 3066 m. This pressure (shown in blue) is where the pressure gradient starts to change. Base on the fact that this point did not recover formation fluids. The Oil Water Contact was set at 3070 m, assuming the transition zone starts at 3066 m.

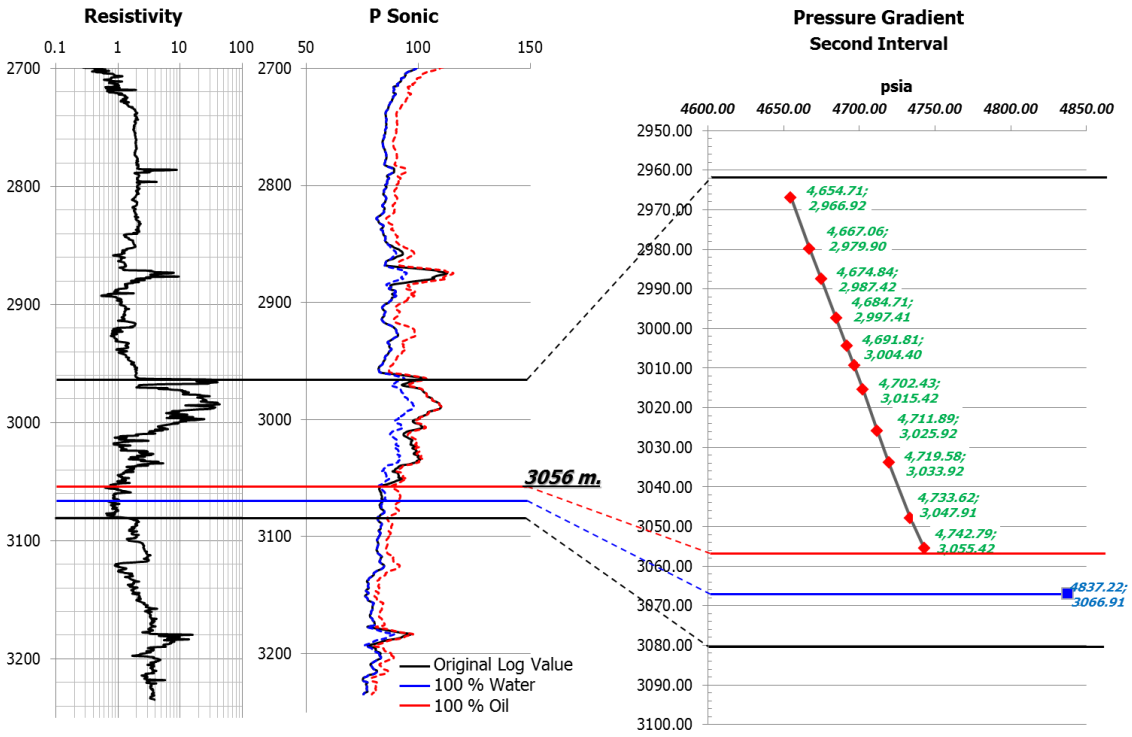

Figure 6-12 MDT Pressure analysis, OWC detected from the gradient pressure change.

6.8. Structural Framework

The geological structural set up of the Beta field is considered to be a dome structure with natural closure in all directions, except to the south of the field where the structure has a closure against salt. This reservoir is characterized also by having a stratigraphic component, since its facies change laterally as shown on the Seismic Attributes section.

The regional structure corresponds to an anticline affected by normal faulting and a direct closure to a salt body present in the South. The salt present in the area is the product of the re activation of the salt diapir as a result this generated the structure. This tramp corresponds to the Middle Pliocene. On the following image (Figure 6-13) the main faults present in the structure are shown, in which faults *F1* and *F_A* are the principal ones. Fault F1 is one of the most important faults in the structure since it is sealing the reservoir sands from the block in the north. This fault has a displacement of approximately 110 meters and the reservoir level is juxtaposing with a sealing formation with the north block.

After analyzing all of the faults with in the structure these faults are found to have a normal displacement. These faults were created due the movement of the allochthonous salt based on the Regional Studies performed by PEMEX in 2011.

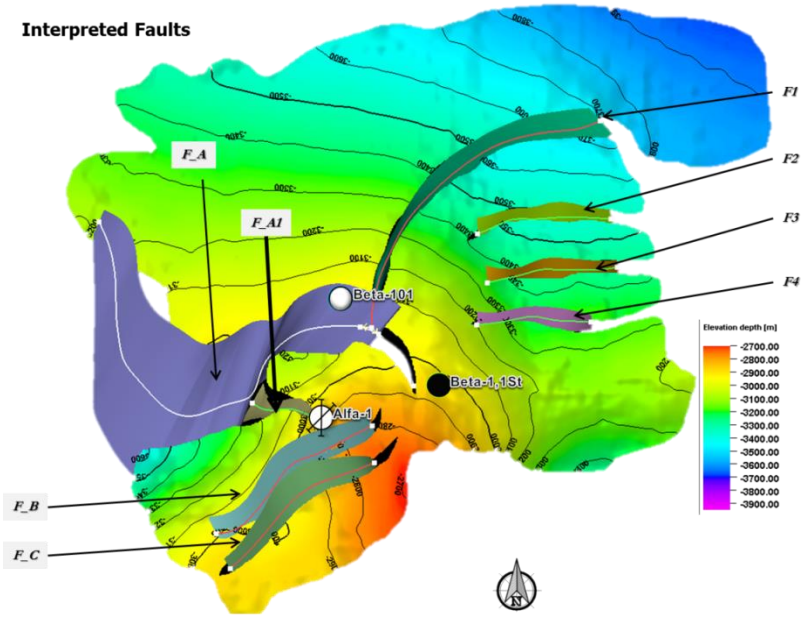

Figure 6-13 Structural Framework Beta Field.

6.9. Seismic Attributes

Since their introduction in the early 1970's, complex seismic trace attributes have gained considerable popularity; first as a convenient display form, and, later, as they were incorporated with other seismically derived measurements, they became a valid analytical tool for lithology prediction and reservoir characterization. (Taner., M., 2001)

The purpose of the seismic attribute analysis is to extract information from seismic data and to provide accurate and detailed information on structural, stratigraphic and lithological parameters. Unfortunately, there are more than three hundred seismic attributes nowadays making it hard to correlate all of them with a specific geological property. This amount of attributes exists mainly because attributes can be generated from Prestack or Postack data.

The following attributes shown on Figure 6-14 to Figure 4-16 where generated from a post stack seismic data set. These attributes where realized focusing on the second reservoir due to the thickness and the possible hydrocarbon prospectivity potential. A different set of time windows were selected over the reservoir two level in order to try to identify possible variations within the reservoir level.

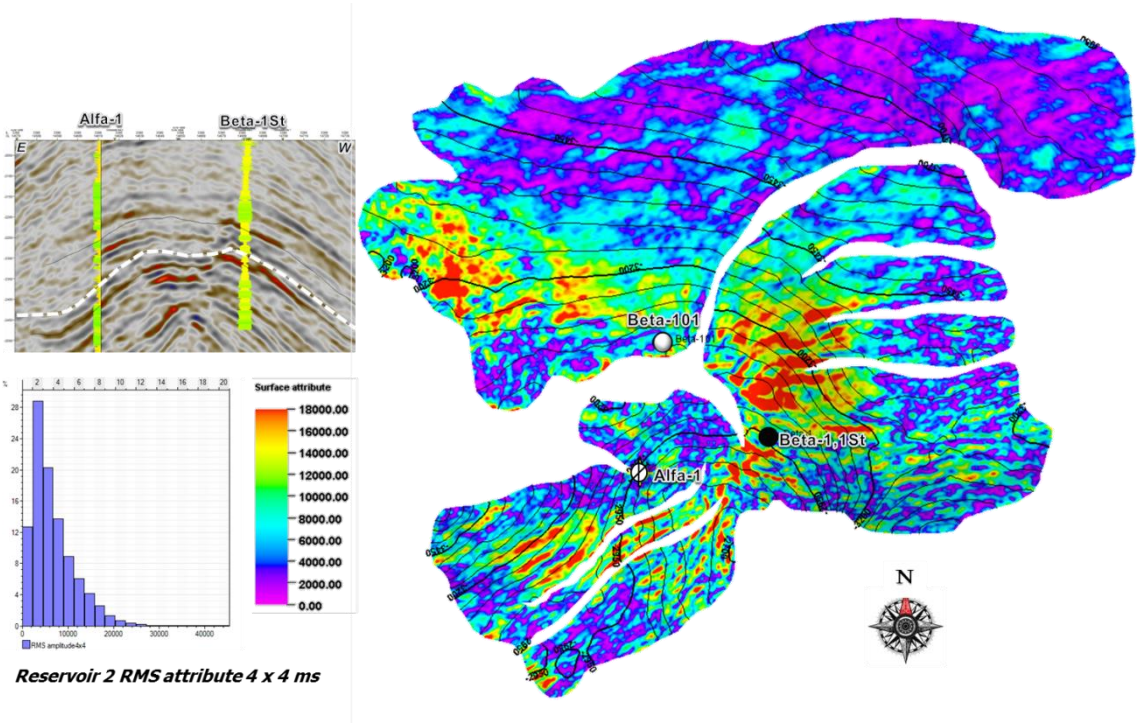

Figure 6-14 RMS seismic attribute, Reservoir two, time window of 4 x4 rms.

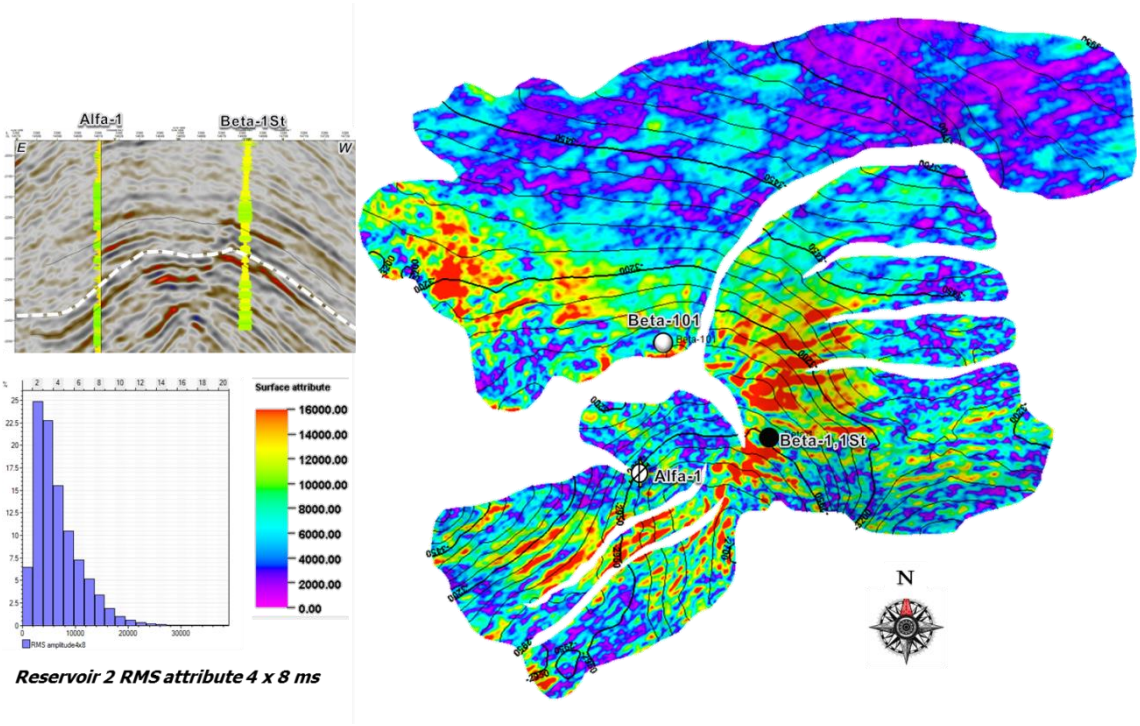

Figure 6-15 RMS seismic attribute, Reservoir two, time window of 4 x 8 ms.

The selected attribute shown on the majority of this chapter is the root mean square or quadratic mean. This decision was made, because this seismic attribute measures the magnitude of variation over a specific data set. Better known as the RMS attribute, it provides information on the variations in acoustic impedance over a sample interval.

A series of different window intervals were selected in order to generate the attributes. Comparing Figure 6-14 and Figure 6-15, it is clear that, in general, the amplitude content within the reservoir level is not varying drastically.

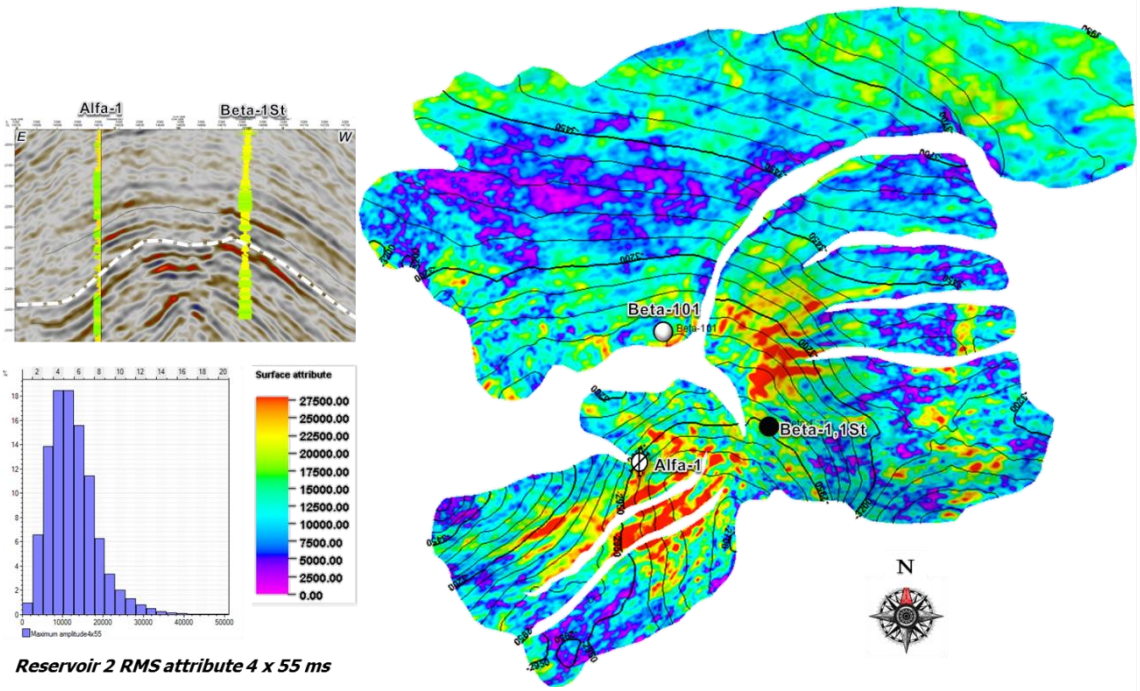

Figure 6-16 RMS seismic attribute, Reservoir two, time window of 4 x 55 ms

The RMS attributes can provide information regarding lithology. For example, a high RMS value in a channel results from either a high acoustic impedance contrast of channel fill with the surrounding environment or acoustic impedance contrast within the infill of the channel (Holdaway 2014) .

From Figure 6-16 it is clear that the high RMS values present on the reservoir level describe a lithology that, in general, has similar properties or similar acoustic impedance values, (similar densities or similar sonic velocities). Based on the attribute, the reservoir level has a considerable lateral extension. In order to corroborate this a different set of attributes were realized. On Figure 6-17 the Variance attribute is presented.

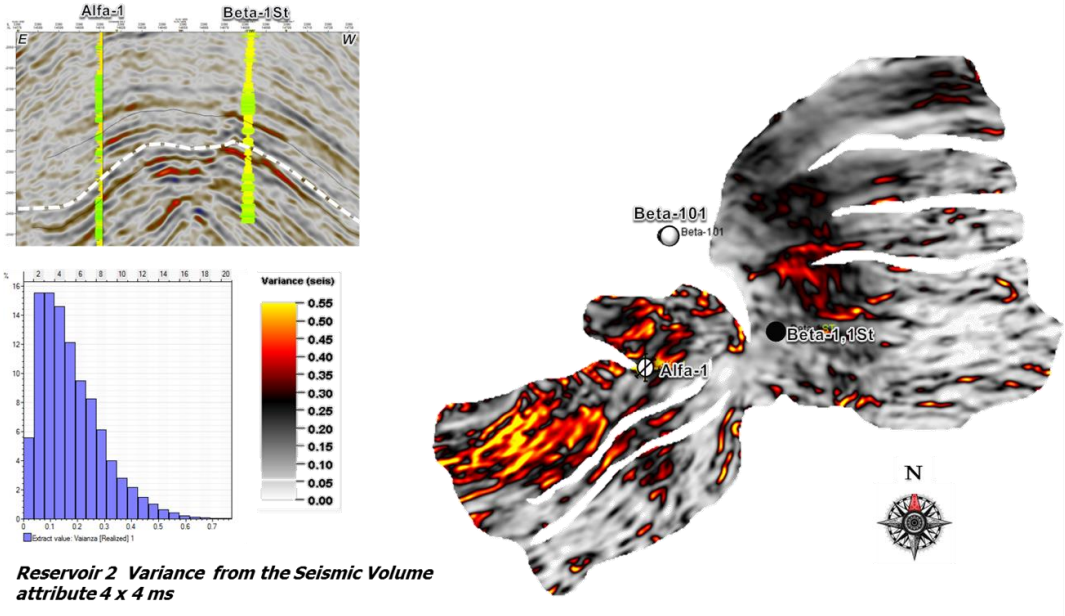

Figure 6-17 Variance attribute, Extracted values over a window of 4 x 4 ms.

This attribute represents the trace to trace variability over a particular sample interval and therefore produces results regarding the lateral changes in acoustic impedances values. Similar traces produce low variance coefficients while difference in traces have a higher coefficients values. This image provides also information regarding the lithology present on the reservoir level. It can be interpreted as an homogeneous reservoir where there are a small amount lateral changes within the reservoir level.

This set of seismic attributes are considered Qualitative attributes. They provide information about spatial patterns as lithological changes or facies changes. It is important to mention that it is essentially impossible to map this attributes directly to a reservoir property such as porosity, and it should not be implemented to quantify reservoir properties (Yilmaz 1987).

7. Petrophysics Calculations

7.1. Introduction

Petrophysical analyses provide the necessary information that is required to generate the STOOIP volumetric calculations and is based on regional geology, the geophysical logs and the core data. Here, we apply a petrophysical analysis to determine a direct relation between the fluids and its movement through the porous media. This relation is determined by analyzing the porosity, permeability, water saturation and mineralogy of the samples.

In this section a brief description of the petrophysical workflow applied in this thesis for the reservoir characterization is presented. This workflow shown on Figure 7-1 includes a porosity model, a water saturation model and a permeability model. The purpose of the Petrophysical calculations is the estimation of the Net Pay.

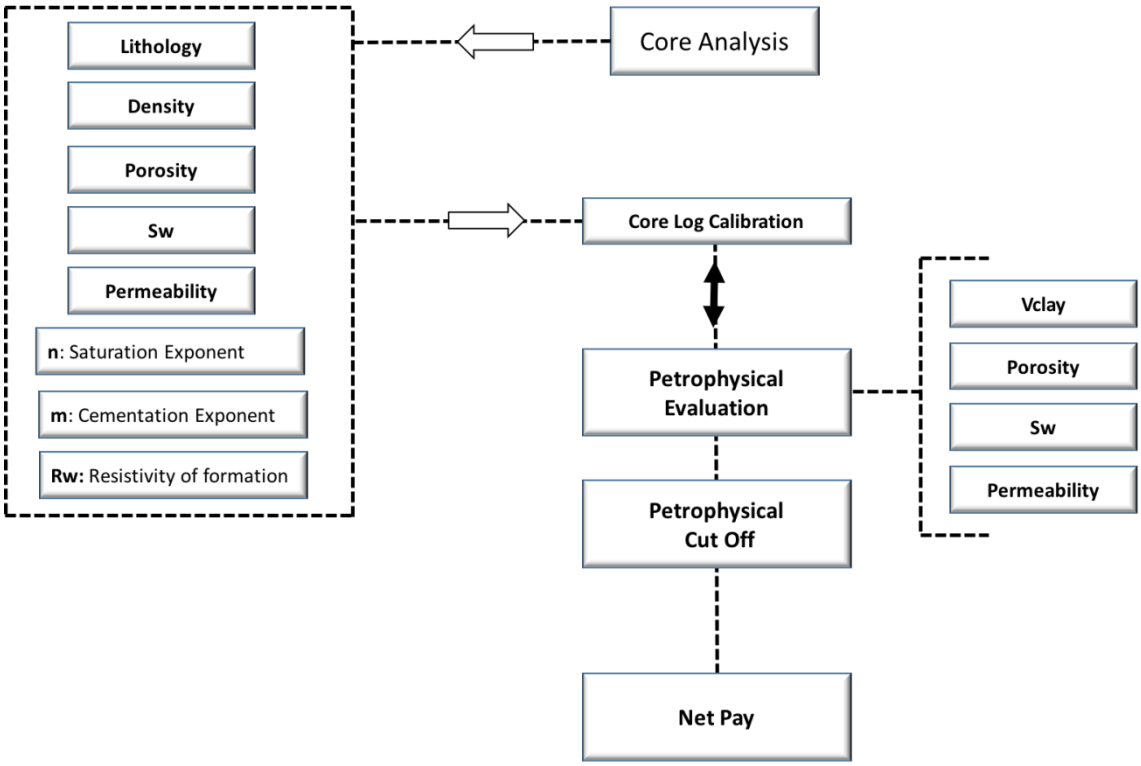

Figure. 7-1 Basic petrophysics workflow. From the core analysis different properties are estimated, they are calibrated with the calculated logs. The final product of the petrophysical evaluation is the estimation of the Net pay.

The following section, is a summary of the core analysis presented in the Geological report. A series of crossplots that represents the reservoirs properties is shown next. From this crossplots, the calculated logs will be compared to ensure the correct values were estimated.

7.2. Porosity-Permeability

The porosity permeability relationship was obtained from core data from the well Beta. The data provided from the core analysis (obtained from the geological report).

Figure 7-1 shows the existing relationship between porosity and permeability of the three different cores identified as (N1, N2 and N3).

From here it is easy to observe that the maximum porosities are approximately 26% and that the second reservoir level represented by the N2 sample presents excellent permeabilities which reach up to 2,000 mD. More commonly however, porosities ranging from 10 % up to 25 %, and the permeability's range from 0.1 up to 1000 mD. It is important to mention that one of the factors that directly affect the relationship between porosity and permeability is the grain size distribution of the sample.

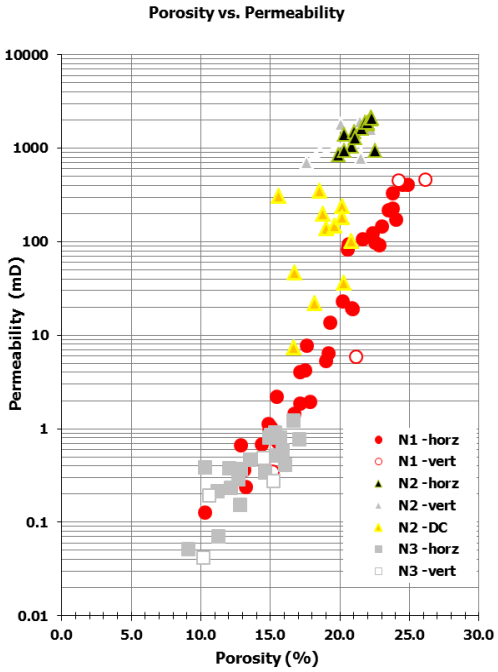

Figure 7-1. Porosity vs Permeability relationship from core data. 3 cores taken from the reservoirs intervals are presented as N1, N2, N3. Horizontal (hortz) and Vertical (vert) permeability values are shown. DC represents the reservoir unit of this thesis.

7.3. Grain Density

By analyzing the grain density of the sample, the density of the rock can be determined. For the sandstones present at the reservoir levels of the Beta well, the density values are on the order of 2.60 gr/cc 2.67 gr/cc. These density values are within the densities ranges of the different wells in the area.

These density values are within the densities ranges of the different wells in the area. The density of the samples can be observed on Figure 7-2. The tree different reservoir units are shown as N1, N2 and N3. The main reservoir unit is the N2.

.

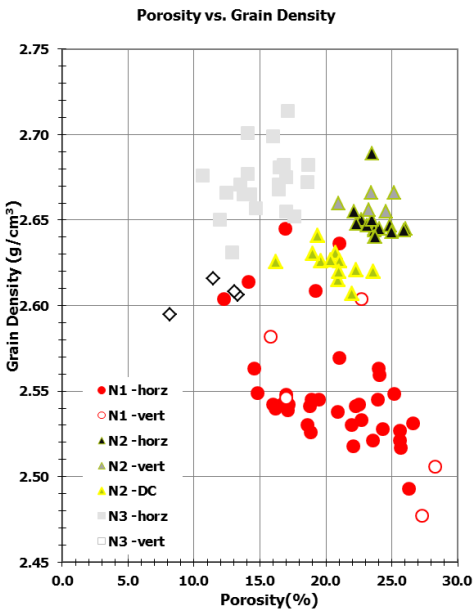

Figure 7-2 Porosity vs Density cross plot from core data

7.4. Petrophysical Model

In order to generate an accurate petrophysical evaluation of the cores, it is necessary to determine a specific set of variables: water resistivity of the formation (Rw), cementation exponent (m), saturation exponent (n), Porosity (Ø), hydrocarbon saturation (1 -Sw) and the permeability (k). All of these parameters will be used in the Water saturation procedure and in the permeability calculations.

The first step in the petrophysical evaluation is to correctly correlate the gamma ray values present in the logs and the values obtained from the cores data.

It is important to mention that the data from the core analysis is already converted to reservoir conditions and depth calibrated. (Figure 7-3).

This depth calibration is an important step since both measurements (logs and core values) should have good correlation in order to correctly calibrate the petrophysical properties. Once the depth is corrected, the correlation between the well and the sample gamma ray values is applied to the other different set of log curves.

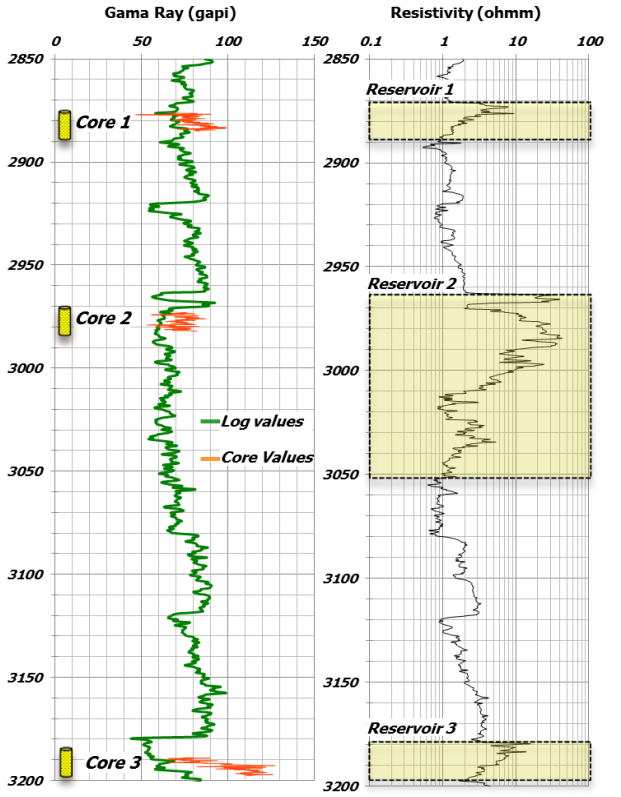

Figure 7-3 Gamma Ray interval of the different reservoir units. The gamma ray log and the gamma ray from the cores is calibrated for the Beta-1.

7.5. Clay volume (Vclay) and Shale volume (Vshale)

The presence of clay minerals in hydrocarbons reservoirs has a great impact on the correct estimation of the final reserves calculation (Ellis et al. 2008). Clay minerals present in shale formations are one of the key factors when estimating porosity, water saturations and permeability's. This is because they are in part controlled by amount of clay minerals present in the pore space (Ellis et al. 2008). This is one of the main reasons why a correct Vclay estimation can generate a correct estimation of the properties, e.g. porosity, that control the quality of the reservoir.

In order to estimate the clay volume, first the Shale volume (Vshale) is calculated. The diference between Vclay and Vshale is that Vclay is focus on the minerals, while the other is focus on the shale content . The Vshale is determined by analyzing the GAPI values present in the gamma ray log. This can be determined by determining the minimum and maximum values of the gamma ray (Asquith, 2004):

$$Vshale = \frac{Gamma\ \ Ray_{log} - Gamma\ Ray_{min}}{Gamma\ \ Ray_{max} - Gamma\ Ray_{min}}$$

Vshale adequately estimates the shale content of the rock. It generally overestimates the clay content (Ellis et al. 2008). The volume of clay can be estimated by the following equation.

$$Vclay = \frac{0.5 * Vshale}{1.5 - Vshale}$$

As mentioned before, the correct estimation of the clay volume is important, since it will be used as an input in the following subsequent Petrophysical calculations. For example, the Vclay will affect the estimation of the effective porosity and the net pay thickness.

7.6. Total and Effective Porosity (Phie)

In order to calculate the effective porosity, it is necessary to estimate the total porosity values. The total porosity is estimated from the values of neutron density ($\emptyset_n$) and density($\emptyset_d$) logs. These values are then corrected using the clay volume. This is shown in the following equations (Asquith, 2004).

$$\emptyset_{Total} = \frac{\emptyset_d + \emptyset_n}{2}$$

$$\emptyset_{effective} = \emptyset_{Total} * (1 - Vclay)$$

7.7. Water Saturation

In order to calculate the water saturation Archie's equation was implemented. This equation relates borehole electrical resistivity measurements to hydrocarbon saturations. It is an empirical law that describes saturation at the reservoir level, using the following equation (Archie, 1942).

$$Sw = \left[\frac{a * R_w}{\emptyset^m * R_t}\right]^{(1/n)}$$

Here *Sw* is water saturation, *a* is the tortuosity factor, *m* is the cementation exponent, n saturation exponent, R_w is the resistivity of the formation water, $\emptyset$ is porosity and R_t is the true formation resistivity derived from the deep resistivity log.

Table 3 Values estimated for the water saturation calculation.

Rw	m	n	a
.034 Ohm	*1.9*	*2*	*1*

The previous parameters are estimated from the core analysis. A brief summary of the parameters is presented. The resistivity of the formation water (Rw) is related to the salinity of the water and the temperatures present in the reservoir. The salinity was estimated from the production test and was set in 90,000 ppm. The cementation exponent (m) models how much the pore network increases the resistivity, as the rock itself is assumed to be non-conductive. The cementation exponent is related to the shape and the distribution of the pore space. The saturation exponent (n) is related to the wettability of the rock and it is determine by an electric properties test during the core analysis (Asquith, 2004).

7.8. Permeability

After the calculation of porosity and the estimation of the sw, the permeabilities can be calculated. Figure 7-2, shows the distribution of permeability values obtained from the core and from calculations using the Timur equation (Timur, 1968).

$$K_{Timur} = \frac{10^4 * (Phi_{effective}{}^{4.5})}{Sw^2}$$

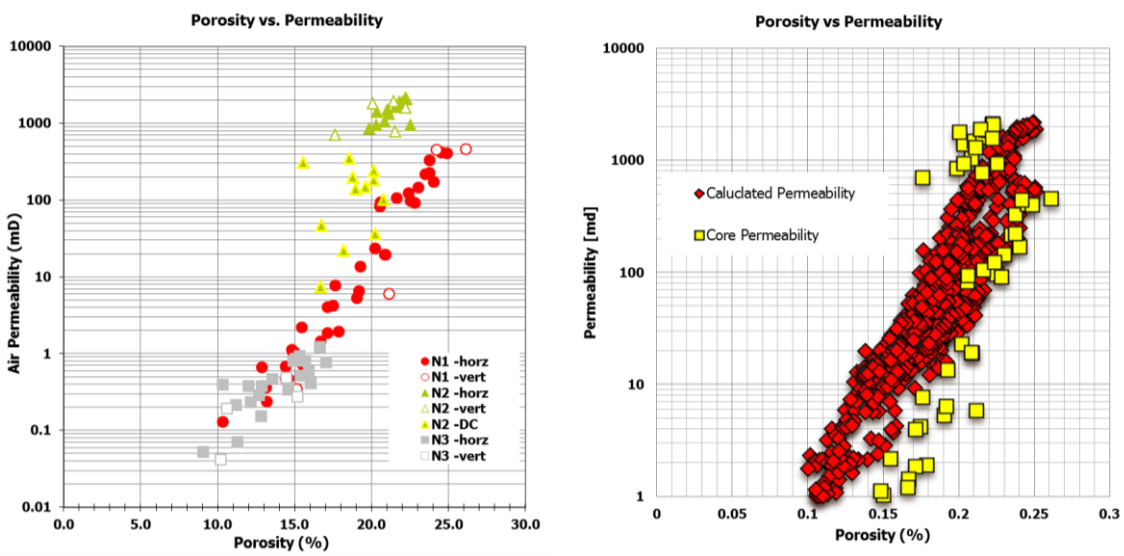

Figure. 7-2 Permeability comparison between the extracted core data and the calculated permeability by Timurs formula. The calculated values are in range with the core data.

7.9. Petrophysical Cutoffs

After the proper calibration of the core data with the estimated log values presented in the previous chapter, the final step in the Petrophysical evaluation is the estimation of the final Petrophysical parameters cutoffs. The cutoff will be applied to the main reservoir unit. The main purpose of the cutoff is to identify the productive from the no productive zones. The result of the petrophysical cutoff is the estimation of the net pay.

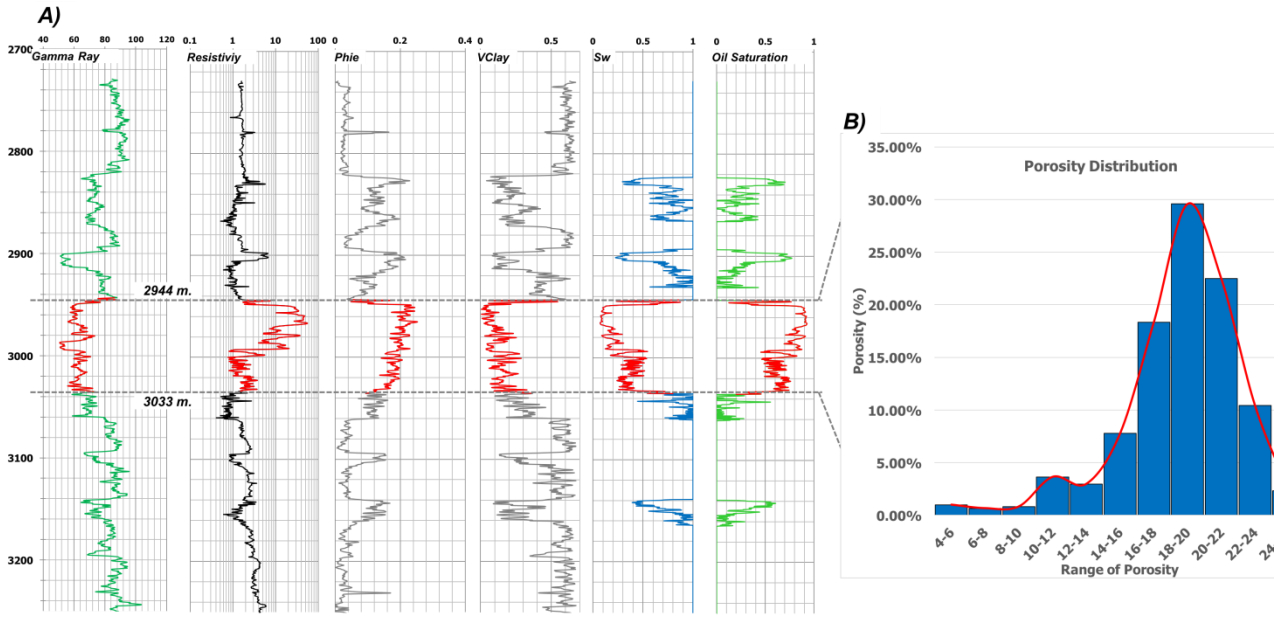

Figure 7-4 A) Geophysical logs Beta-1St second reservoir level. The main interval is defined between the depths of 2944 and 3033m. B)The average porosity in the main interval defined as 18%.

The selected reservoir level to be evaluated in this section corresponds to the second reservoir level, which is defined from 2944 m to 3033 m. The Petrophysical evaluation is presented on Figure 7-4 A). This interval has an average porosity (phie) of 18% as shown on Figure 7-4 B) . The average values of porosity, water saturation and vclay were also estimated. For this interval the average water saturation is 30%.

As previously stated, the purpose of the Petrophysical evaluation is to find the appropriate reservoir properties to determine if a reservoir unit is productive. Based on the average values of porosity, water saturation and vclay. These parameters are put into pore volume estimation in order to see how these parameters affect the volumetric.

It was estimated that the cutoff parameters to be used in the Petrophysical evaluation are as follow :

Phie ≥ 12 % Sw ≤ 45 % Vcl ≤ 40 %

By applying these cutoff parameters, the net pay can be calculated. Net Pay is a key parameter in reservoir evaluation because it identifies the reservoir intervals that have sufficient reservoir quality and significant hydrocarbon content in order to considered a producing interval.

The results of the net pay calculation based on the above shown cut-off values are presented in Figure 7-5. The results show that the total Net pay intervals have a thickness of 77 meters, (the initial thickness was estimated as 89 meters, as indicated by the red lines in the graphs of Figure 7-5.

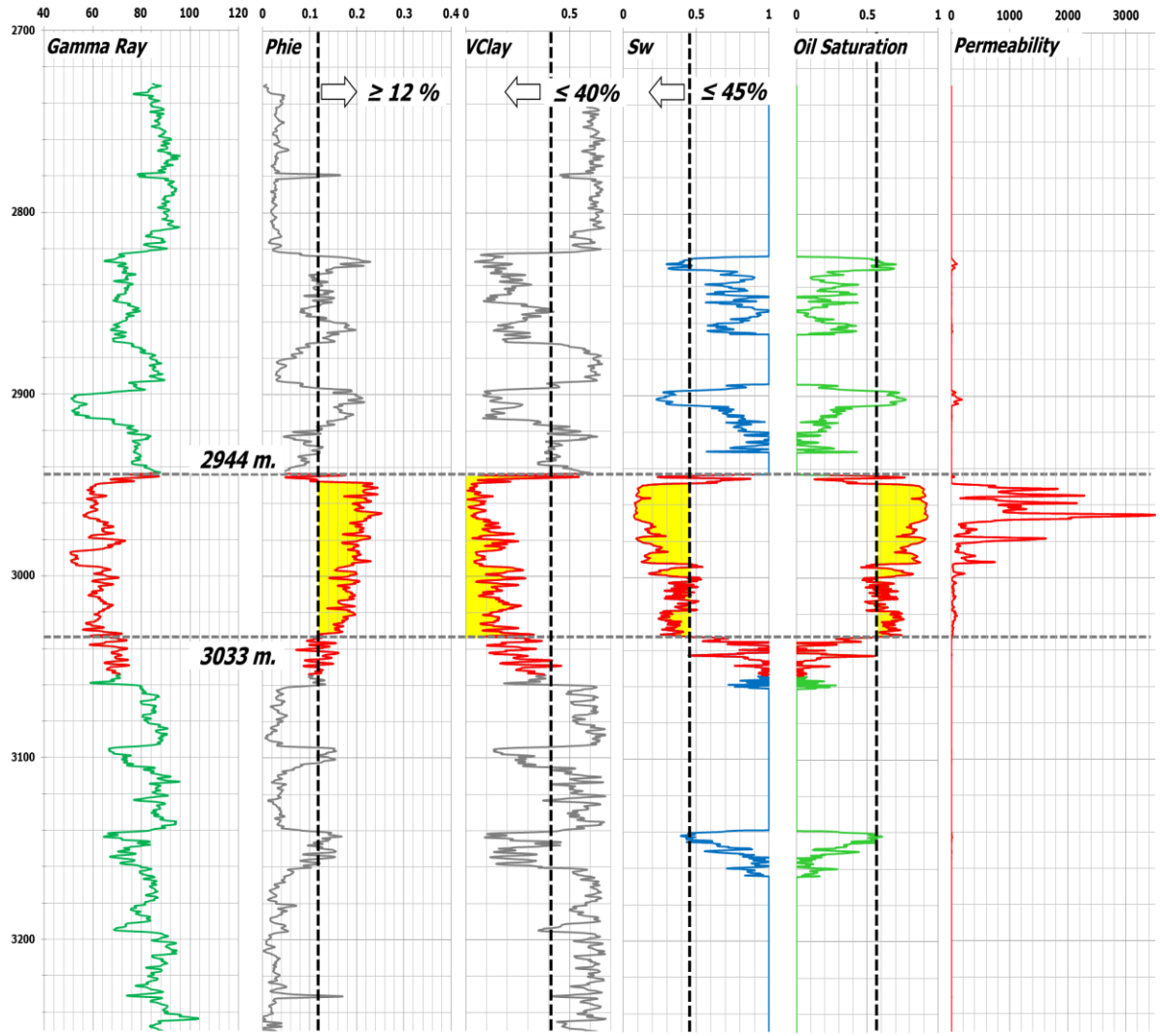

Figure 7-5 Petrophysical Evaluation with cutoff of Porosity, Sw and Vclay

8. 3D Property Modelling

The property model workflow involves several processes in which the most important are: Fault modeling, Upscaling the well logs, Facies Modelling and Petrophysical modelling. This series of processes have the main purpose of extrapolating the values presented in the well logs and populating the grid cells based on the values presented on the well data (Adeoti 2014) . This process starts by generating a 3D grid, in which each cell of this grid will be populated by the original well data values.

It is important to mention that the property modelling is a key part of the characterization process, since several properties will be use to generate volume calculations and, in some cases, mathematical Petrophysical properties; for example the generation of Sw (water saturation) as a property volume.

8.1. Fault Modeling

Fault modeling is the process where faults are modeled with the intention that these faults will form part of the final 3D grid Model. This is realized during the Pillar gridding process (Figure 8-1). These pillars will be inserted in between the faults with the purpose of having a pillar in every grid cell that is intercepted by a fault.

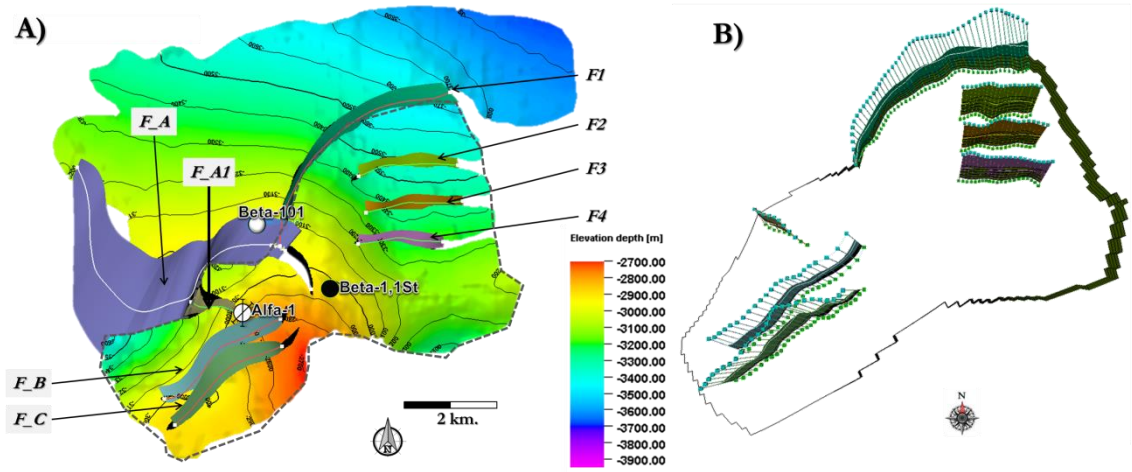

Figure 8-1 A) The main faults interpreted on the reservoir level map. B) Pillar Gridding and modelling of faults. The modeling of the faults only corresponds to the area close to the Alfa and Beta well (dotted line in A)

8.2. Upscaling

Upscaling is the process of assigning the well log values in to the 3D grid cell. These values will be valid only for one cell of the model and it will be assigned to the zone that has been cut by the well. This process has the purpose of using the well data set as an input for populating the 3D property model.

8.3. Facies Modeling

Once the 3D structural framework has been created and the sequences (reservoir units) identified, the internal bedding geometries are defined within each sequence. The layering schemes define lines of correlation inside the model and are used to laterally connect facies and, ultimately, the Petrophysical properties. The next step is to model the facies and simulate their 3D spatial distribution. The facies previously discussed on (The Depositional Environment Chapter), were obtained from the analysis of the available geological data. A series of cores corresponding to the Beta well reservoir levels where analyzed. Based on this analysis, the different reservoir units were defined as lower shoreface and middle shoreface.

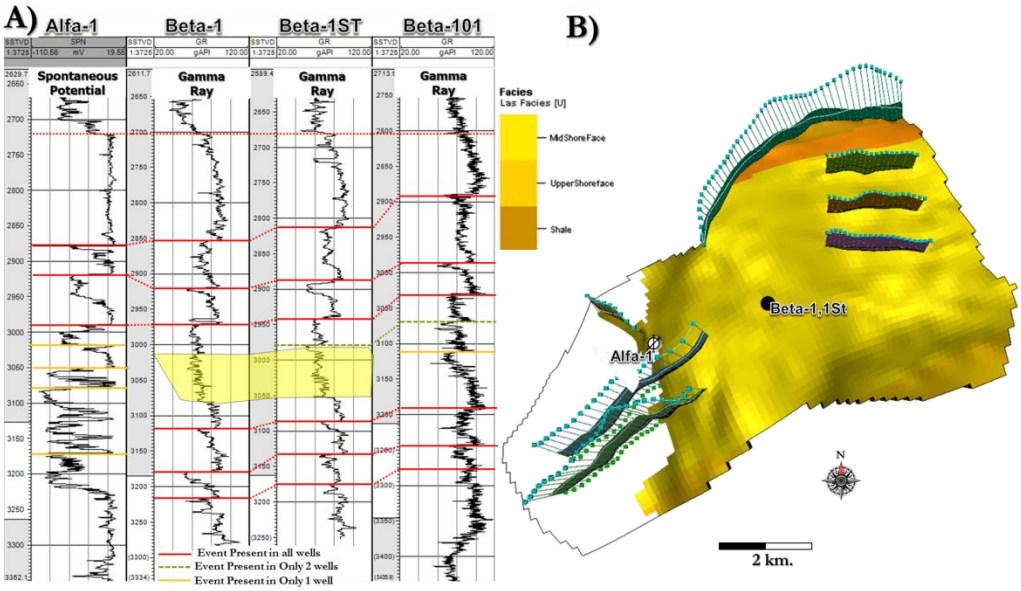

Figure 8-2 Final Facies Model based on the analysis performed in the wells, where the reservoir 2 unit, does not laterally correlates to the events present in the Alpha well. This can be observed in the A), the interpreted body does not reach the Alfa well. B) The final facies model represents the no continuity of the reservoir unit.

As previously mentioned on the previous chapters. It was established that the depositional environment corresponds to a wave dominated delta. Based on the well correlation between the wells present in the area. The Figure 8-2 A) shows a well correlation in were the gamma ray is displayed. It is clear that the gamma ray behavior of the Alfa well corresponds to a different geological setting. Based on the log data, it can be interpret as being closer to a distributary channel this due the spiky gamma ray behavior. In the other hand, the gamma ray behavior of the Beta-1 and Beta-st are rather similar, this can be explained by interpreting the gamma ray behavior between the wells as the same depositional environment, thus it can be interpreted as the same sand package.

From this behavior, it can be interpreted that not all of the sand bodies present in the reservoir levels are laterally connected between the Alfa and Beta wells this is shown in the interpreted sand Figure 8-2 A). On the B) section of the image, the final facies model is presented. The Middle shoreface facies is set for the Beta wells and the facies is laterally limited based on the information of the well correlation and the seismic attributes.

The selected method to generate the Facies modeling was an Stochastic algorithms, an object base model was used. This method generate realizations of geological objects with available geometric data (Aigner, 2007). From the correlation of the logs shown in Figure 8-2 A) the lateral extension of the reservoir unit was determined, and based on the information of the seismic attributes, the areal distribution was determined. This information was used for the object base, facies model.

8.4. Porosity 3D model

Porosity is one of the most important rock properties in describing porous media. It is defined as the ratio of pore volume to bulk volume of a rock sample. The most important use of the porosity is to quantify the storage capacity of the reservoir, and, from this estimate the amount of hydrocarbon present that potentially can be produced. The first property modelled from the well data was the porosity volume. In order to correctly estimate the lateral and vertical distribution of porosity in the reservoir, a Stochastic 3D property modelling technique was used. In this case, a Stochastic distributions method, called Gaussian Random Function Simulation (GRFS). This method is characterized by simulating a variable guided by a second variable. The (GRFS) is a faster and robust method compare to the traditional Sequantial Gaussian simulation (Daly et al. 2010).

This method was selected because it calculates a value with the highest probability for each point, using variograms and the property distribution of the input data. Property models generated with this methodology look more reasonable than those modeled using deterministic averaging methods and they honor the input distribution data more realistically. The main disadvantage related to this methodology is that far away from the know data, the method generates realistic results (Daly et al. 2010). One way to overcome this downside of the modelling technique, is by using a second property as a trend.

As mentioned before the selected distribution method, is characterized by having the ability to model properties that are to some extent related to other properties. The porosity model in this case will be guided by a second property that is related to it. In this case the second property used as a trend is the Acoustic Impedance. Different researchers have shown the direct relationship between porosity and acoustic impedances (Goodway et al. 1997, Cemen et al. 2014, Osman et al. 2014)

P impedance values determined from the 3D seismic inversion data set can be used to locate the zones of low and high porosities in sandstone reservoirs, this has been shown on the work done by Dahlberg et al. 2000. This relationship between the acoustic impedance and porosity can be seen in Figure 8-3. A cross plot is presented between Porosity and acoustic impedance, this cosplot corresponds to the Beta-1St reservoir level. The color property corresponds to water saturation. This cross plot provides a linear correlation between the acoustic impedance and the porosity present in the log. The zones corresponding with higher porosity values within the reservoir correspond to low impedance values within the reservoir unit.

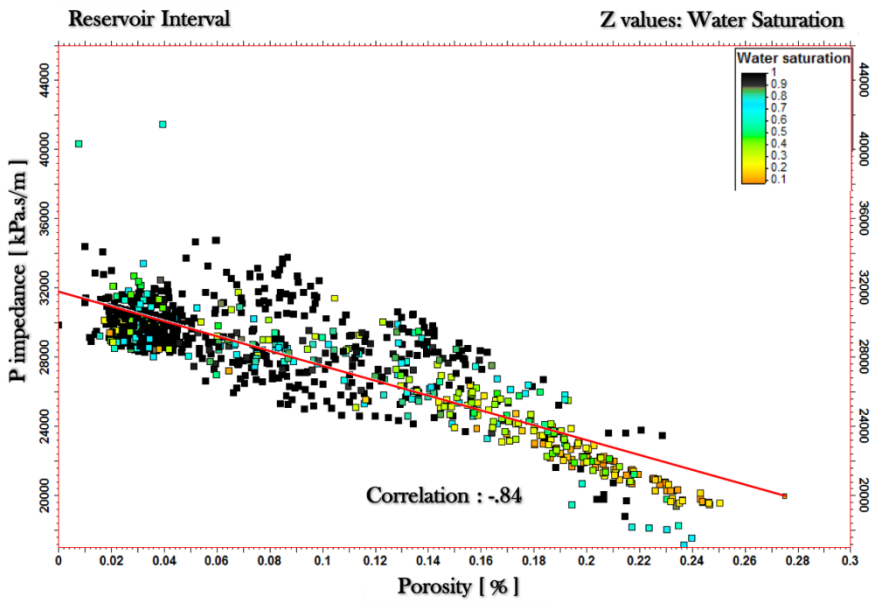

Figure 8-3 Porosity vs Impedance cross plot, this corresponds to the Beta-1St in color the water saturations are shown, in where the darker colors represent water content.

The P impedance volume can be used as tool to better understand the reservoir unit away from the limited well control, reducing the possibility of generating fake results elsewhere from the control point. Due to the good correlation presented within these two properties, the acoustic Impedance volume was used as a second property to guide the 3D porosity distribution. The correlation presented in Figure 8-3 corresponds to the reservoir interval, this correlation behavior is assumed to be present away from the well control. As the reservoir is considered a low acoustic impedance, the low impedance areal distribution is known from the extracted seismic attributes.

This was realized first by converting the P impedance volume, that is originally in time into depth. This conversion was done using the layer cake velocity model discussed on the Geophysics chapter. Once the volume is in depth, it will be used as a trend to guide the Porosity Model. This is realized during the Gaussian Random Function Simulation (GRFS) in where the estimated the relationship between the two different properties will be applied. This is realized under the Co-Krigin option. Cokriging can be described as a multivariable estimation method, this is because this method deals with two or more attributes within the same field. Cokriging methods uses the relationship between properties that are related (Olea 2012), in this case the first property is known in the well but the second property is present in the area. This is where the correlation between the two properties becomes important, since having a value of zero correlation means that the two properties have no correlation and having a value means a 100% correlation.

On the next Figures the final porosity volume is shown, and also a comparison is shown between generating a model with and without the help of the Acoustic Impedance property Trend.

The second interval corresponding to the zone with better reservoir quality shown on (Figure 7-5) was divided in two different intervals. This was decided due to the thickness of the layer, since making only one layer, will not allow to see vertical changes on the estimated properties, it was decided to generate a division on the interval layer. The final porosity model resulting from the implementation of the Acoustic impedance volume as a trend (Figure 8-4), has similarities to the seismic attributes of the second interval. This suggests that the Gaussian facies model technique used for elaborating this property modelling is properly distributing the porosity values encountered by the Beta well, and laterally populating the 3D model.

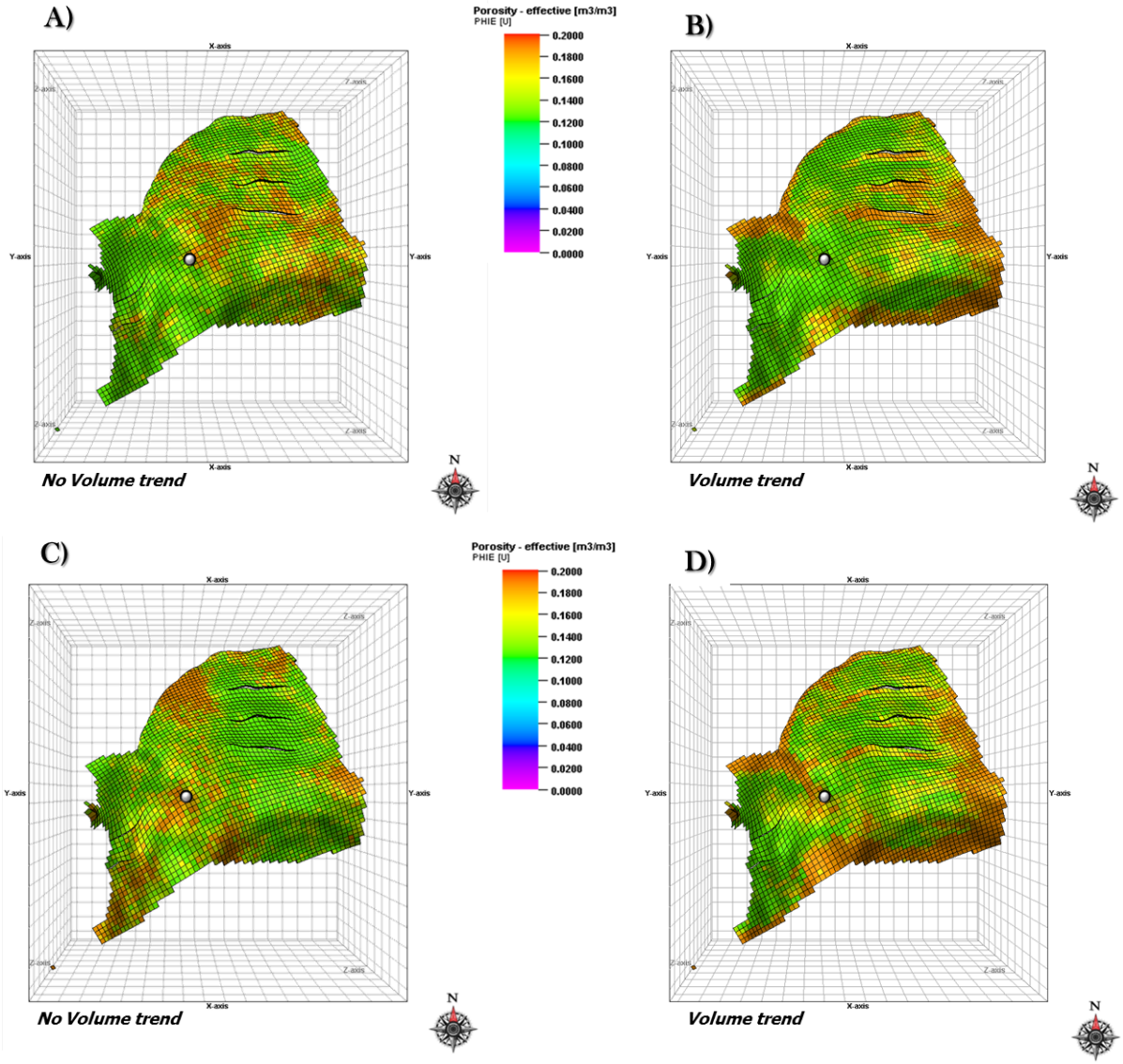

Figure 8-4 Comparison of the Porosity property modeling of the Reservoir level. Figure A) and B) corresponds to the upper part of the reservoir unit. Figure C) and D) correspond to the lower part of the reservoir unit. The comparison between using the second trend as a guide is made, a better result is obtained by using the Acustic impedance as a trend.

8.5. Water Saturation Petrophysical 3D model

Calculating water saturations (Sw) has been, for many years, the key step for estimating volumetric calculations in the oil industry (Baker et al. 2015). The correct mapping of water saturation in zones away from the well is the main purpose of saturation height modeling. Saturations height functions are important as these can highly influence the STOIIP (Stock Tank Oil Initially In Place) calculations for a reservoir.

Before starting the water saturation property modeling, there are many methods for estimating the water saturation functions available in the literature (e.g. Leverett 1941., Johnson 1987., Cuddy 1993., Skelt 1995.).

The main purpose of the Sw property modeling is to predict the water saturation anywhere within the reservoir level above the free water level. Depending on the depth in the reservoir level, there will be a different oil saturation which will vary as we get closer to the free water level. The free water level can be expressed as the zone in where the oil and also the water phase show a similar pressure behavior.

This zone, in which the water saturation varies with height, is controlled by the capillary pressure. The capillary pressure is unique to the geologic formation since it reflects the interaction of rock and fluids, and is predominantly controlled by the pore geometry, sorting of the pores, interfacial tension and wettability (Tenente., 2015).

From the geological report and the core analysis report a capillary curve was constructed which provides the necessary information regarding the water saturation present in the reservoir interval. Figure 8-5 shows the results from the core analysis.

From this curve we are interested on the behavior of the Drainage curve. This curve represents the process when hydrocarbon migrates into a reservoir and displaces water. From this figure we can observe that the water saturation present in the reservoir level decreases with increasing height above the free water level (FWL), where capillary pressure is zero.

As previously discussed in the (Figure 6-12) the free water level was estimated to be at 3070 m.

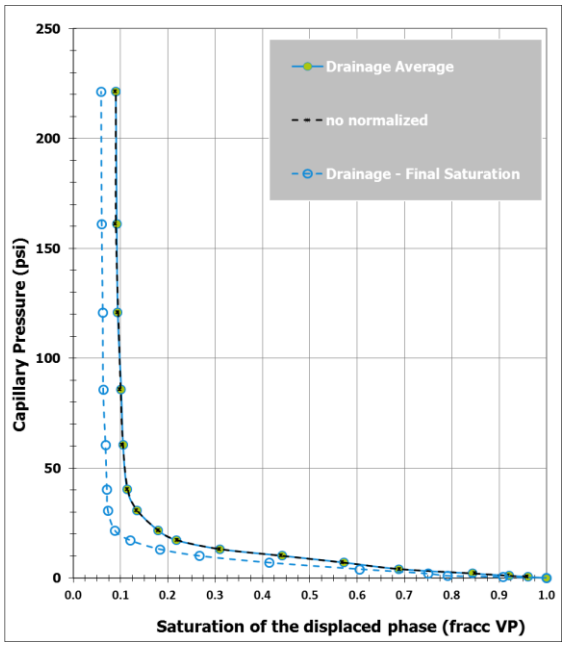

Figure 8-5 Drainage and Imbibition curves performed to the core plugs of reservoir 2. This is taken from the geological report data.

In order to generate the water Saturation 3D property it's important to understand how the capillary pressure is changing in relation with the distance from the free water level (Figure 8-5). The selected function to generate the water saturation property is the Lamda Function shown on the following equation (Al-Bulushi et al. 2010). This is a mathematical function that uses curve fitting algorithms on the existing log data specifically the porosity log.

$$Sw = aPc^{\gamma} + b$$

Where

$$\gamma = c\theta + d$$

The different coefficients in the lambda function are obtained from a linear regression analysis methods from the calculated water saturation, porosities and the height from the free water level. The parameters a,b,c and dm are fitting functions used to obtain the water saturation (Wiltgen 2003). The resultant water saturation as a function of the height above the free water level for a range of different porosities is shown in Figure 8-6. The curve in black and red is the one associated with the porosity present in the core data measurements for the reservoir level, the other curves show different scenarios in where the behavior of the water saturation function while changing the porosity.

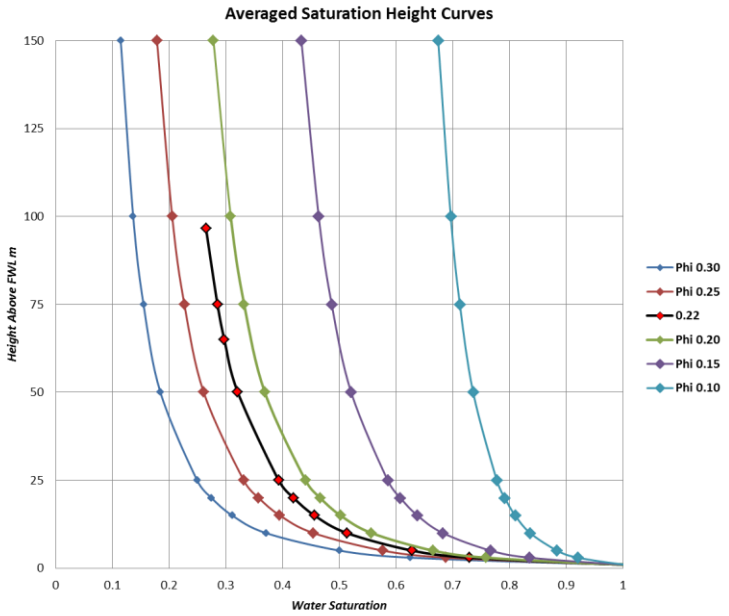

Figure 8-6 Calculated water saturation function based on the height of the Reservoir, in black with red is the curve that fits the porosity of the reservoir.

9. Quantitative Seismic Interpretation

As previously discussed in in the geophysics section, the objective of conventional seismic interpretation is the mapping of structures in the subsurface. This seismic interpretation cannot be considered as a quantitative method. It is considered qualitative because it provides information regarding the shape of structures in the subsurface. In order to obtain a real quantitative interpretation, a different approach has to be taken into account.

The future in the interpretation techniques is the interpretation of Elastic impedance volumes. This new approach is achieved by seismic inversion. Seismic trace inversion it characterized by reducing the effect of the wavelet by replacing the seismic amplitude with calibrated impedance traces. This provides information regarding the acoustic layering in the subsurface (Latimer et al 2000).

Acoustic impedance is expressed as the product of the density of the rock and P-wave velocities, it is considered a rock property and not an interface property as seismic reflection data. Connolly (1999) defined Elastic Impedance "as a function of P wave velocity, S wave velocity, density, and incidence angle. To relate Elastic Impedance to seismic, the stacked data must be some form of angle stack rather than a constant range of offsets.". Goodway et al (1997) proposed a method to extract more rock properties. On his work he explains the use of the relationship between the lamé parameters λ (Incompressibility), μ (rigidity) and ρ (density) .

$$\lambda = Vp^2 * \rho - 2Vs^2 * \rho$$

$$\mu = Vs^2 * \rho$$

In the research done by Goodway, it is demonstrated that LMR (Lambda-Mu-Rho) approach can be used to separate lithologys and identify fluids. Mu-Rho (μ) or rigidity is defined as the "resistance to strain resulting in shape change with no volume change" (Goodway et al. 1997). This parameter is very useful for lithology discrimination and is related to the rock matrix.

Lambda-Rho λ, or incompressibility, is a very useful parameter to distinguish fluid content which is subjected to pore fluid. A number of studies have found that a sandstone containing hydrocarbon is less dense than a sandstone containing water and also are more compressive than wet sandstone. As a result, in a sand reservoir containing hydrocarbon the Lambda-Rho (LR) log shows low λ incompressibility values.

For the realization of this thesis work, a set of elastic impedance volumes is available.
The seismic inversion was done using Jason RockTrace Inversion for P-Impedance and S-Impedance. The inversion project was calibrated with five wells, these wells went through a strict Rock Physics workflow. Rock Physics relate porosity, mineralogy saturation, and pore fluid properties to the elastic rock properties, providing the connection between seismic impedance and velocity inversion and physical reservoir properties. Four of the wells used in this inversion have reservoir units.

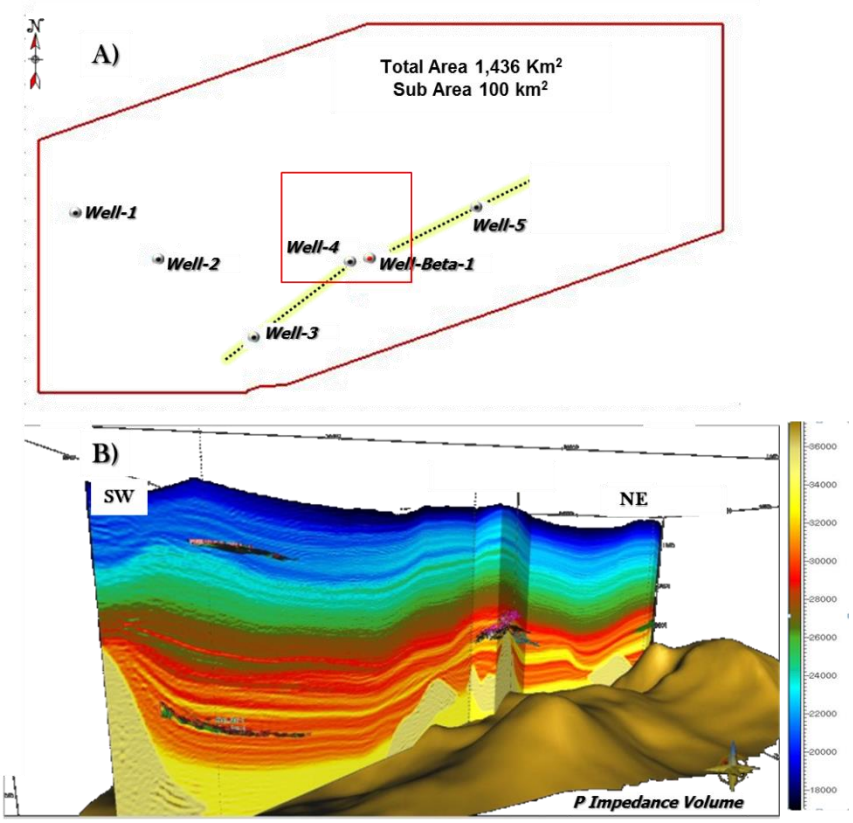

Figure 9-1 A) Seismic Inversion study area used for the reservoir characterization 100 km2. B) A Regional section of the P impdance cube, the direction of the line is shown in the yellow line.

This study was realized over an original area of 1,436 km2 and a sub volume of 100 km^2 was used for this thesis work (Figure 9-1), the interval of interest covers the depths approximately 2500 m to 3500 vertical depth. Due to coverage considerations at these depths, the maximum offset used in the inversion is 4500. Based on a previous AVO analysis of the area, the anomalies present in the beta field is considered a class III AVO sands in the reservoir interval, while the Alfa well showed no AVO anomaly. (Figure 12-4). A set of eight offset sub stacks ranging from 101 to 4500 m where used to generate the well tie. From this well tie a series of Amplitude Varying with the Offsets wavelets were extracted for each sub stack, an average wavelet representative of each sub-stack was extracted and used in the final inversion step.

This seismic inversion features the incorporation of a low frequency model for P velocity, S velocity and Density. The importance of this low frequency model is to merge the ultra-low frequency range present in the logs in to the missing low frequency range of the seismic data. All the wells have measured p and s sonic logs and all the wells were used to generate the low frequency model.

The offset stacks, the averaged wavelets, the five wells and the low frequency model are the inputs for the Seismic Inversion. The main output of this seismic inversion is a set of P impedance and S impedance elastic volumes used for the identification of hydrocarbon anomalies in the study area. A general workflow of this seismic inversion is shown on the Appendix.

As mentioned, this seismic inversion was realized by using a set of wells present in the area, this wells have gone through a severe Petrophysics and Rock Physics workflow. This is one of the key steps in the entire seismic inversion workflow. This step will allow to describe a reservoir rock by physical properties such as porosity, rigidity, compressibility; this properties that will affect how seismic waves physically travel through the rocks.

On the following image, a set of cross plots between different elastic parameters are presented. With the help of this cross plots it is easier to identify the zones corresponding to the reservoir levels. These areas correspond to the area delimited by the yellow zone. As shown on (Figure 6-5), our main reservoirs present a low impedance, as well a low s impedance value, on Figure 9-2 some of the elastic parameters corresponding to the different reservoir levels are shown.

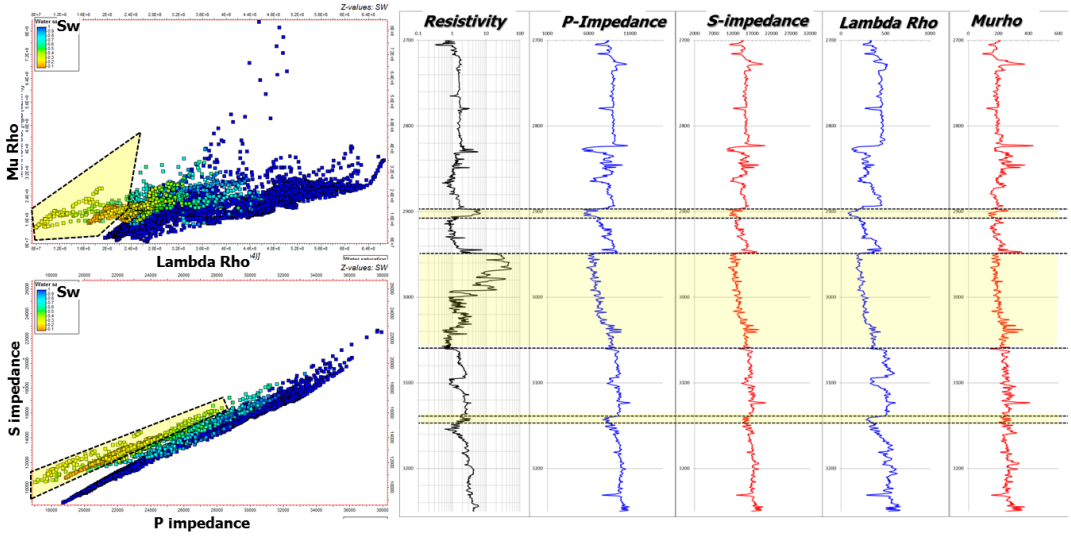

Figure 9-2 Cross plot of a different set of elastic impedances, and a set of logs containing the different elastic parameters.

In order to correctly integrate the quantitative criteria to the reservoir characterization process, the elastic impedance volumes were analysed and a set of attributes were derived in order to observe and to have a correct estimation of the lateral extension of the Fluid present on the reservoir level.

The following image is an RMS attribute realized in the second reservoir interval level. Figure 9-3 shows the distribution of the fluids corresponding to the second reservoir. From this attribute is important to mention that the attributes shows no fluid content on the Alfa well, this is consistent with the information provided by the logs in which this well was classified as dry.

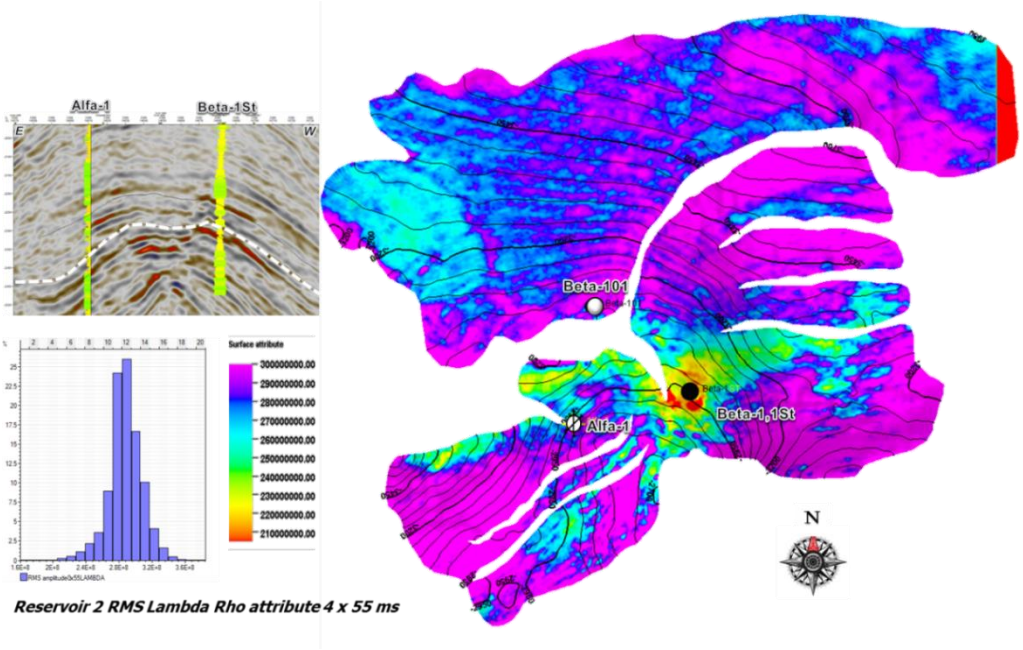

Figure 9-3 RMS attribute derived from the elastic volume Lambda Rho. The low values shown in the attribute can be directly associated to fluid presence.

10. Volumetric Calculations

The final stage of the reservoir characterization is the estimation of the original oil in place, better known as OIIP. This OIIP volume calculation is a measurement used in characterization studies that are intended to evaluate the potential economic value of a reservoir unit. This equation is determined from properties present in the reservoir and reservoir fluids, and has the purpose of providing a measurement of the amount of oil that is present in the reservoir. This calculation is shown by the following equation (Baker et al. 2015).

$$OOIP = \frac{Area * h * \emptyset * (1 - S_w)}{B_{oi}}$$

The volumetric calculations dependents on: porosity (Phie), thickness of the reservoir (h), the area of the reservoir that is usually contoured from maps of the reservoir properties areal extension (Area), B_{oi} is the formation volume factor and the Hydrocarbon saturation (Sw). The final result from this equation is given in barrels (a unit of volume for crude oil that is equivalent to 159 litters or 42 gallons).

This calculation takes into account the fact that not all of the oil in the reservoir can be extracted. The percentage of oil volume that can be extracted from the reservoir is controlled by the Recovery factor. This factor has to be applied for the difference between the volume of the same mass of oil in the reservoir to its volume when brought to the surface,. Based on analysis of producing fields near the Beta field area, a recovery factor of .25 was assumed.

The last parameter from the OOIP equation is the Formation Volume Factor of Oil Boi. This parameter is defined as the volume change of oil between reservoir conditions and surface conditions.. This change in volumetric results from the pressure drop between reservoir conditions and surface conditions. This is due to gas expulsion from the oil as pressure is decreased (McCain 1990).

From the petrophysical evaluation of the second reservoir unit, the following reservoir values where obtained: the Average Porosity is estimated to be 18%, average Water Saturation 22%. After the application of the selected Petrophysical cut offs (*Phie ≥ 12 % Sw ≤ 45 % Vcl ≤ 40 %*). The reservoir level initially defined between the depths of 2944 m to 3033 m, estimated to have 90 meters of good reservoir rock quality, was properly corrected resulting in a Net Pay thickness of 77 meters.

The estimated area of the reservoir was obtained from the Seismic Attributes section and was calculated to be 4.71 Km^2. This area is delimited by the Oil Water Contact found in the Pressure plots at 3070 m. This contact is shown on the amplitude map by the white lines Figure 10-1. By using these conventional seismic attributes the main assumption made is that the RMS amplitude attribute is responding to a lithological change, and it is not related to fluid content.

The following image (Figure 10-1) shows the volumetric calculation in which an estimated original oil in place of 246.40MMbls (million barrels) is obtained. From this calculation, after the application of the recovery factor an estimated reserve of 61.60 MMbls (million barrels) is estimated.

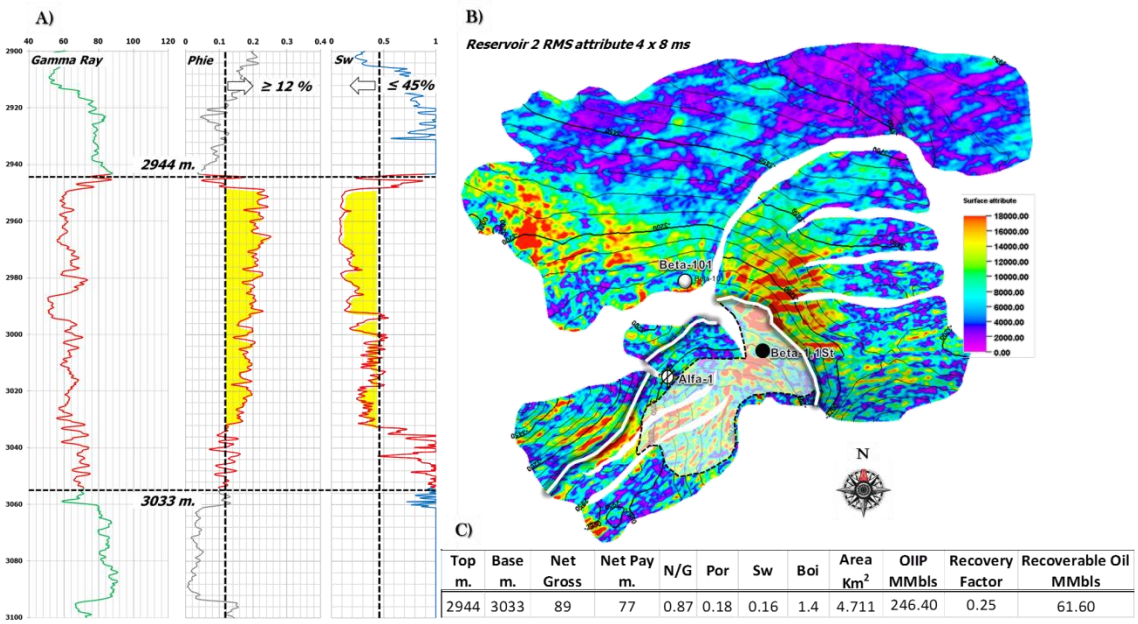

Top m.	Base m.	Net Gross	Net Pay m.	N/G	Por	Sw	Boi	Area Km^2	OIIP MMbls	Recovery Factor	Recoverable Oil MMbls
2944	3033	89	77	0.87	0.18	0.16	1.4	4.711	246.40	0.25	61.60

Figure 10-1 Volumetric calculation of the second reservoir level, this volume calculation was realized by using traditional seismic attributes maps to obtain the area, this was delimited by the OWC.A) Petrophysical evaluation of the reservoir unit. B) RMS attribute map of the reservoir unit, this attribute proportionate an lithological anomaly with an estimated area of 4.711 km. C) Volumetric calculation.

A second reserve estimation case scenario was generated in order to proportionate a more strict fluid distribution map. In this second estimation the use of the seismic inversion volumes will be implemented. This scenario is based on quantitative seismic methods. The Lambda Rho attribute is used to provide map of fluid anomaly distribution (Fig 10.2) which shows an anomalous area of 3.7 km^2. The final estimated Recoverable Oil based on this map is 45 MMbls.

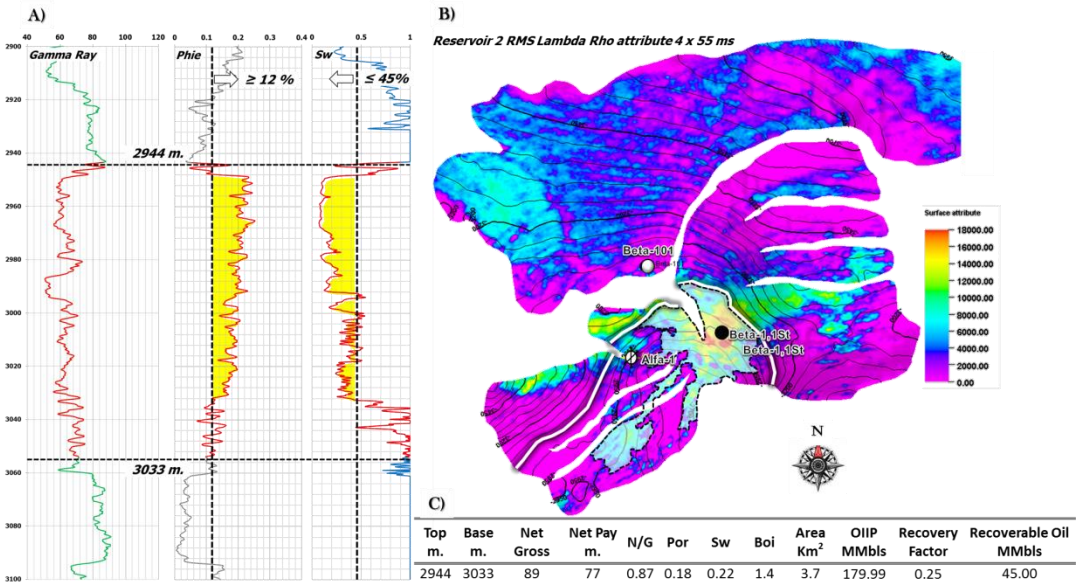

Top m.	Base m.	Net Gross	Net Pay m.	N/G	Por	Sw	Boi	Area Km^2	OIIP MMbls	Recovery Factor	Recoverable Oil MMbls
2944	3033	89	77	0.87	0.18	0.22	1.4	3.7	179.99	0.25	45.00

Figure 10-2 Volumetric calculation of the second reservoir level, this volume calculation was realized by using Quantitative Seismic Attributes maps to obtain the area, This maps shows the distribution of the fluids present in the reservoir unit. A) Petrophysical evaluation of the reservoir unit. B) RMS attribute map of the reservoir unit the attribute corresponds to the RMS of the Lambda Rho volume, this attribute proportionate a fluid anomaly with an estimated area of 3.7 km. C) Volumetric calculation.

In order to achieve a more accuracy, and to understand which parameter has most impact on the final reserve estimation, an uncertainty analyses was performed. Here, a range of values were selected for each of the inputs, Net to Gross, Porosity, Sw Area and Recovery factor. The range of the input values is based on the minimum and maximum values encountered within the reservoir unit of this specific parameter. The parameters of the sensitivity analysis can be observed on Table 4. The final results of the sensitivity analysis is observed on Figure 10-2.

The image shown on (Figure 10-3) is an example of how the range of the input parameter 'area' was selected. The minimum area was estimated from the overlap of the estimated area from the traditional seismic attribute Figure 10-3 A) this area is associated to a lithology response. Figure 10-3 B) shows the response of the quantitative attribute that its correlated to fluid distribution. In order to reduce the uncertainty and to obtain a minimum area for the sensitivity analysis. Figure 10-3 C) shows the overlap of the two estimated areas, and it represents the zone in where lithology and fluid generate overlaps. The minimum area was determined (2.35 km^2) red dotted line.

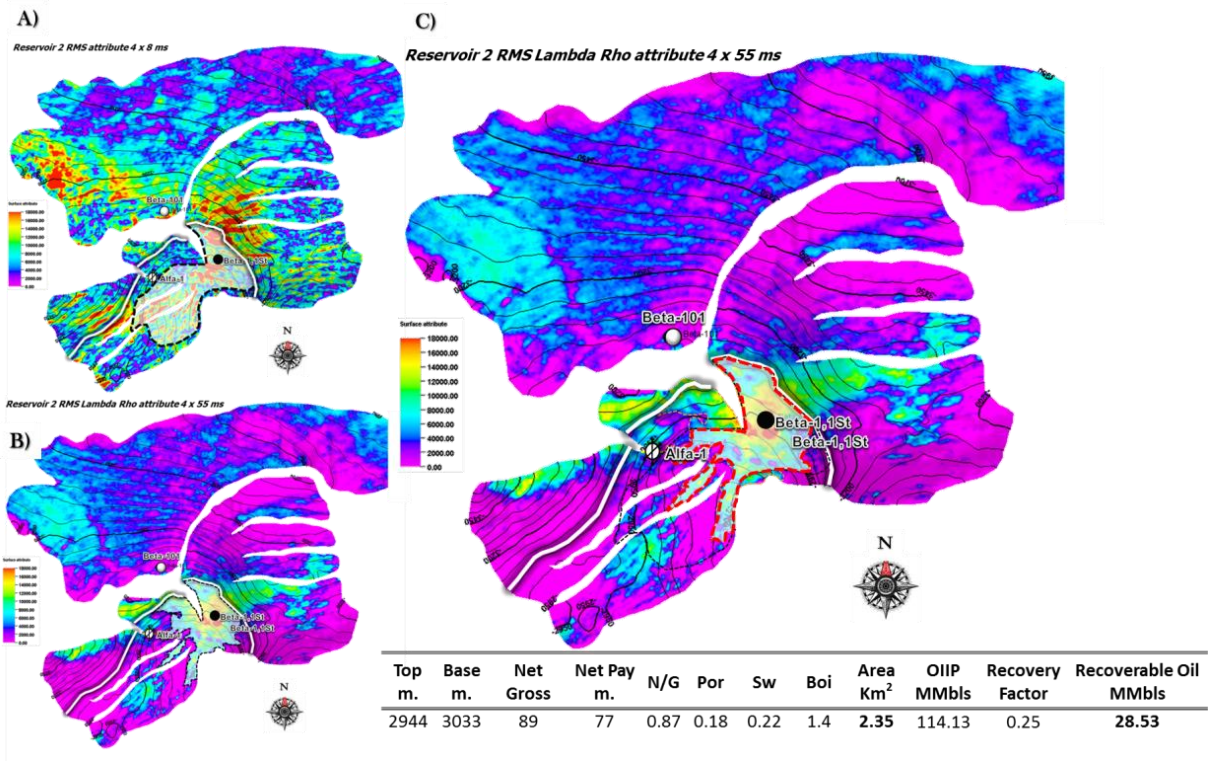

Top m.	Base m.	Net Gross	Net Pay m.	N/G	Por	Sw	Boi	Area Km^2	OIIP MMbls	Recovery Factor	Recoverable Oil MMbls
2944	3033	89	77	0.87	0.18	0.22	1.4	**2.35**	114.13	0.25	**28.53**

Figure 10-3 Different areas estimated from traditional seismic attributes(A) and quantitative seismic attribute(B) The minimum estimated area is shown on the right in where the overlapping areas of both attributes give a minimum area of 2.35 km2.

Table 4 Parameters for sensitivity Analysis.

Area Km^2	Rf	N/G	Por	Sw	Recoverable Oil MMbls
2.35	0.18	0.6	0.14	0.16	
2.95	0.2	0.65	0.16	0.18	
3.7	0.23	0.75	0.17	0.2	
4.711	**0.25**	**0.87**	**0.18**	**0.22**	**57.20**
4.8	0.27	0.9	0.19	0.24	
5	0.3	1	0.2	0.26	

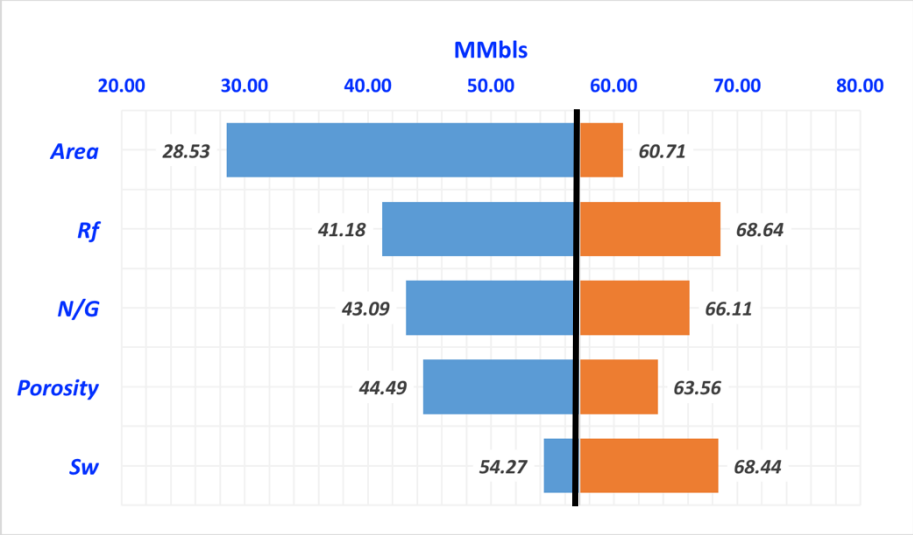

Figure 10-4 Sensitivity Analysis.

Once the volumetric calculations were realized using the OIIP equation, the final step was to compute the volumetric calculation. This calculation takes into account the petrophysical properties volumes that were calculated in the previous chapters. The results of the final volumetric calculation is shown in the next table.

Table 5 Final volumetric calculation.

*Bulk volume [*10^6 m3]*	*Net volume [*10^6 m3]*	*Pore volume [*10^6 rm3]*	*STOIIP (oil) [*10^6 sm3]*	*Recoverable oil [*10^6 sm3]*
371	323	58	34	9

N/G	*Por*	*So*	*Sw*	*STOIIP (oil) [*MMbbls]*	*Recoverable oil [*MMbbls]*
0.87	0.18	0.79	0.21	213.82	**56.60**

The final volumetric estimation for the second reservoir unit was estimated to be 56.6 MMbbls of Recoverable Oil. The distribution of the Recoverable oil is shown in Figure 10-5 C. Here, the area of the reserves is shown by the dotted white line. This area is delimited by the OWC, and it has an area of 3.95 km^2. The figure also shows that the estimated area of recoverable oil overlaps both, the lithology indicator seismic Attribute (Fig 10-6B) and also the quantitative attribute indicating the presence of fluids (Figure 10-6A).

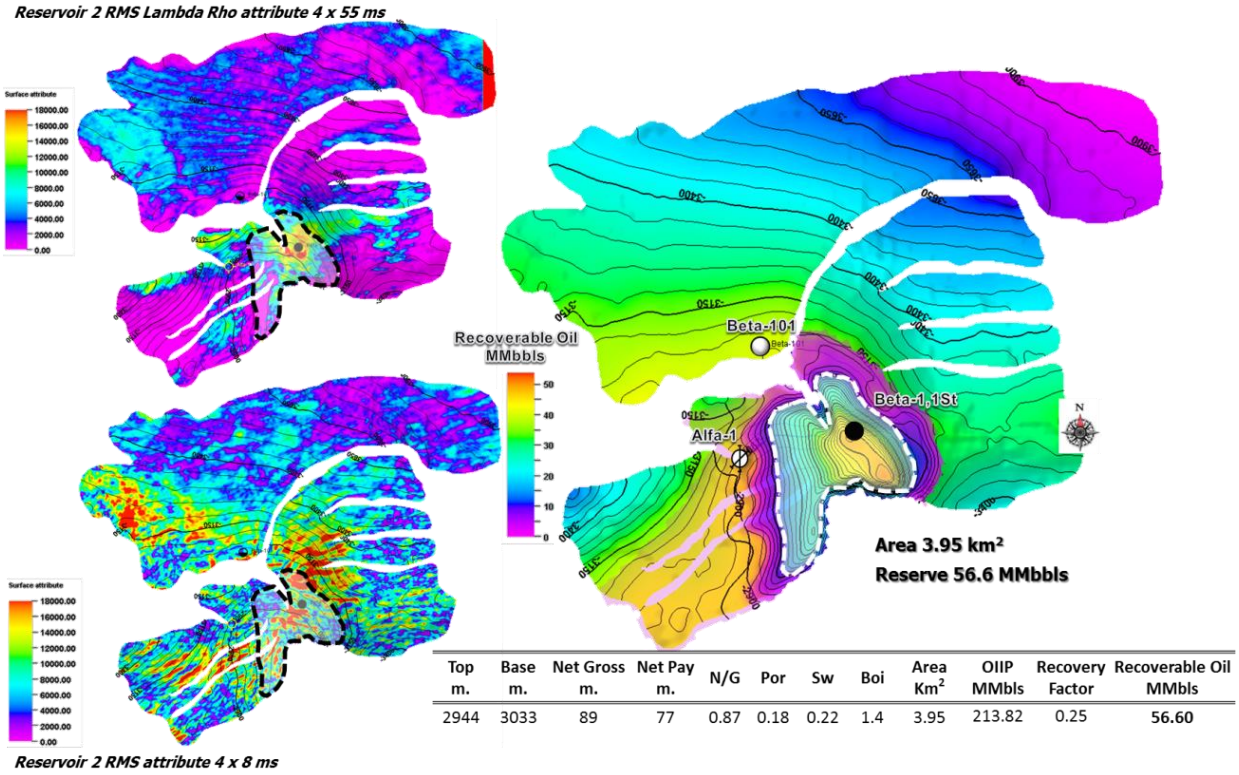

Top m.	Base m.	Net Gross m.	Net Pay m.	N/G	Por	Sw	Boi	Area Km^2	OIIP MMbls	Recovery Factor	Recoverable Oil MMbls
2944	3033	89	77	0.87	0.18	0.22	1.4	3.95	213.82	0.25	**56.60**

Figure 10-5 Final volumetric estimation, area of recoverable oil is estimated in 3.95Km2.

11. Conclusions

The focus of this study is the characterization of the Pliocene plays located within the Istmo Saline Basin in the shallow southeastern Gulf of Mexico. An workflow was developed in order to properly characterize the geological and sedimentary features of the reservoir based on detailed analyses of the available data, such as cores, seismic data and geophysical logs.

Core data revealed grain size distributions, sedimentary structures such as cross bedding and hummocky cross stratification and vertical grading trends which were used to interpret the paleo depositional environment. The main reservoir unit is interpreted to represent a wave-dominated delta with coast parallel beach ridges and associated feeder channels. This interpretation was used to correlate the available wells into a cross section revealing a proximal to distal trend in depositional environment and grain size.

The next step was an initial phase of traditional 3D seismic interpretation, including well to seismic matching. This allowed the correct identification of the reservoir unit in the seismic volume. With the help of the geophysical logs, and once the reservoir unit was properly positioned in the seismic data, the interpretation phase for the main reservoir level was initiated. The interpretation of the structures in the subsurface was continued by a structural interpretation phase including the identification of faults ending in a depth conversion of the reservoir level.

Once the internal structure of the reservoir was known, the next step was to understand the lateral extent of the reservoir. The implementation of elastic parameters derived form a seismic inversion is a powerful tool for the detection and delimitation of hydrocarbons. This phase was initialized by the generation of cross plots between the relevant rock properties of the reservoir unit and the elastic parameters obtained from the seismic inversion. These cross plots were used to identify the fluid content in the reservoir unit. Finalizing the quantitative phase with the elaboration of quantitative seismic attributes that allowed for the correct identification of the lateral extension of the reservoir.

Based on the geological and geophysical data, key petrophysical properties were obtained focussing on the reservoir unit. The correct estimation of Porosity, Water saturation, Net to Gross, Vclay content and Permeability is a key step for the reserves calculation. All of these parameters were obtained base on the log data and and core analysis. A series of calibrations were realized in order to corroborate the estimated properties. This was done after the estimation of all of the Petrophysical parameters of the reservoir unit in order to properly estimate the reserves present in the field.

Based on the Petrophysical cut offs, the vertical and lateral extent of the reservoir unit was identified. These cutoffs are the following *(Phie ≥ 12 % Sw ≤ 45 % Vcl ≤ 40 %).* The reservoir level in the Beta field was defined between the depths of 2944 m and 3033 m, with a Net to gross of 89 meters and a net pay of 77 meters. A series of traditional seismic attribute maps were realized in order to estimate the areal distribution of the reservoir rock. Additionally the use of seismic attribute maps derived from the elastic parameters allowed for the correct delimitation of an area containing the hydrocarbons present in the field. These two areas were used in the volume calculations. Finally, once the properties of the reservoir units where acquired, the areas obtained from the attribute maps were used to provide a range of possible scenarios for the reserve estimation. The final reserve calculation for the beta field was estimated to have 56 MMbls of Recoverable oil in place distributed over an area of 3.95 km^2.

Overall the main contribution to the reservoir characterization workflow proposed in this thesis, is the use of seismic inversion derived rock property volumes. These volumes have proven to determine the lateral extension of the reservoir unit, as shown by the quantitative seismic interpretation section. The implementation of this newly added workflow step, considerably reduces the uncertainty during the delimitation stage of newly discovered fields, especially for fields that have no clear evidence of an Oil Water Contact. More importantly the use of these elastic impedance volumes, not only benefited the interpretation of the reservoir unit, but it was of significant guidance during the creation of the static model, as one of the main 3D property model was guided by the relationship between P impedance and porosity. The benefits from the proposed workflow is represented by ensuring a more accurate and successful volumetric estimation, that in the long run will provide a risk reduction when drilling and developing new wells in the field.

12. Appendix

12.1. Sedimentary Texture Analysis Theory.

In this section, different aspects regarding the internal structure of the samples will be discussed. The principal characteristics, like the shape of the clasts, grain size and the degree of sorting, are all aspects of the texture of the material. By using the scale shown in Table-6, called the Wentworth scale (Wentworth, 1922), the different grain sizes will be determined from the core plugs of the well cores.

Table 6 Wentworth scale of rock sizes from the publication: Chester K. Wentworth in a 1922 article in The Journal of Geology: "A Scale of Grade and Class Terms for Clastic Sediments".

Classification		Particle Size (diameter)
Gravel	*Boulder*	*> 256 mm*
	Cobble	*64 mm – 256 mm*
	Pebble	*4 mm – 64 mm*
	Gravel	*2 mm -4 mm*
Sand	*Very coarse sand*	*1 mm – 2 mm*
	Coarse Sand	*.5 mm -1 mm*
	Medium Sand	*.25 mm - .5 mm*
	Fine Sand	*.125 mm -.25 mm*
	Very fine Sand	*.0625 mm - .125mm*
Silt	*Coarse Silt*	*.031 mm - .0625 mm*
	Medium Silt	*.0156 mm - .031mm*
	Fine Silt	*.0078 mm - .0156mm*
	Very Fine Silt	*.0039 mm - .0078 mm*
Mud	*Clay*	*< .00006 mm*

“For the shape of the clast is important to notice that the roundness of the sample is achieved by the abrasion of the clast surfaces when coming in contact with each other during the sediment transport”(Nichols 2009). Generally, the roundness of the clasts is visually determined using charts based on Pettijohn et al.1987, as shown below.

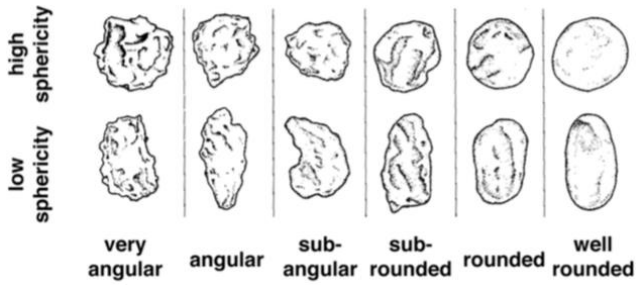

Figure. 12-1- Sphericity chart based on Pettijohn et. al. 1987.

The sphericity radio of the clast is the main indicator of the transported distance. With increased transport distance, the samples tend to be more rounded. A visual estimate of the sorting is shown in the following Figure.

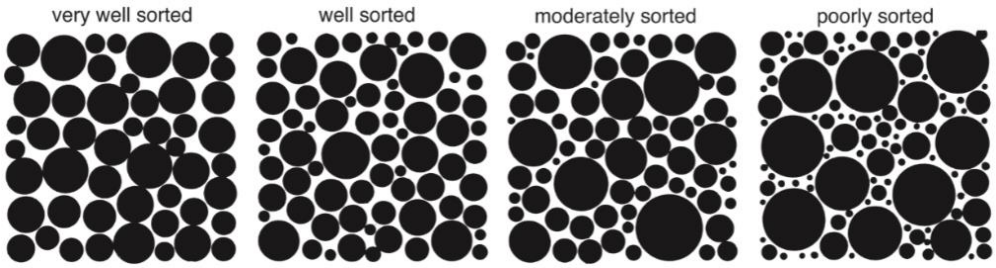

Figure. 12-2 Chart providing a visual tool to estimate the sorting of the samples. (taken from**Invalid source specified. **)

12.2. Core Sample

Figure 12-1 Core Fragment example.

12.3. Seismic Processing Workflow.

The main basic processing steps realized to the seismic volumes is shown next. The seismic data used in the elaboration of this thesis it's a seismic sub-volume from this data set. Next the most relevant steps taken during the processing stage are presented:

- Trace basic editing and Geometry check.
- Noise attenuation (random and lineal).
- Amplitude stripes attenuation (De-striping) using the Q methodology.
- MERGE OF THE SEISMIC VOLUMES
- Multiple attenuation by the Radon Method.
- Regularization and Interpolation.
- Migration velocities selection.
- PreSTM Migration by the Kirchhoff method.
- Attenuation of lineal noise using the FK filter.
- Amplitude Compensation.
- Application of the RMS residual velocities and Random Noise attenuation.
- Amplitude Scaling.
- Merging of the seismic Volumes.

12.4. Layer Cake Velocity Model

Table 7 Velocity Model Layer Cake

Well 1								Verification of velocity choice	
Horizon	Interval	TWT	Depth	Cum. OWT	Interval OWT	Interval thickness	Velocity [m/s]	Interval thickness	Diff. Well data [m]
Seabottom	-	0	0	0					
Layer 1	1	730	722	365	365	722	1978	712	-10
Layer 2	2	979	1015.42	489.5	124.5	293.42	2357	286	-7
Layer 3	3	1750	2069	875	385.5	1053.58	2733	1064	10
Layer 4	4	2100	2620	1050	175	551	3149	560	9
Layer 5	5	2300	2962	1150	100	342	3420	330	-12
									-10

Horizon								Verification of velocity choice	
Horizon	Interval	TWT	Depth	Cum. OWT	Interval OWT	Interval depth	Velocity [m/s]	Interval thickness	Diff. Well data [m]
Seabottom	-	0	0	0					
Layer 1	1	730	722	365	365	722	1978	712	-10
Layer 2	2	980	1016	490	125	294	2352	288	-7
Layer 3	3	1870	2253	935	445	1237	2780	1228	-9
Layer 4	4	2133	2675	1066.5	131.5	422	3209	421	-1
Layer 5	5	2290	2950	1145	78.5	275	3503	259	-16
									-43

Horizon								Verification of velocity choice	
Horizon	Interval	TWT	Depth	Cum. OWT	Interval OWT	Interval depth	Velocity [m/s]	Interval thickness	Diff. Well data [m]
Seabottom	-	0	0	0					
Layer 1	1	690	664	345	345	664	1925	673	9
Layer 2	2	1010	1050	505	160	386	2413	368	-18
Layer 3	3	1750	2105	875	370	1055	2851	1021	-34
Layer 4	4	2100	2703	1050	175	598	3417	560	-38
Layer 5	5	2250	2948	1125	75	245	3267	248	3
									-79

12.5. Final interval Velocities

Table 8 Final Velocities used for the selected intervals.

Interval velocities [m/s]					
Well	**Int. 1**	**Int. 2**	**Int. 3**	**Int. 4**	**Int. 5**
1	1978	2357	2733	3149	3420
2	1978	2352	2780	3209	3503
3	1925	2413	2851	3417	3267
Max. difference in velocity [m/s]	53	61	118	269	237
(Weighted) average	1960	2374	2788	3258	3397
Interval velocity [m/s]	**1950**	**2300**	**2760**	**3200**	**3300**

12.6. Rock Fluids Workflow

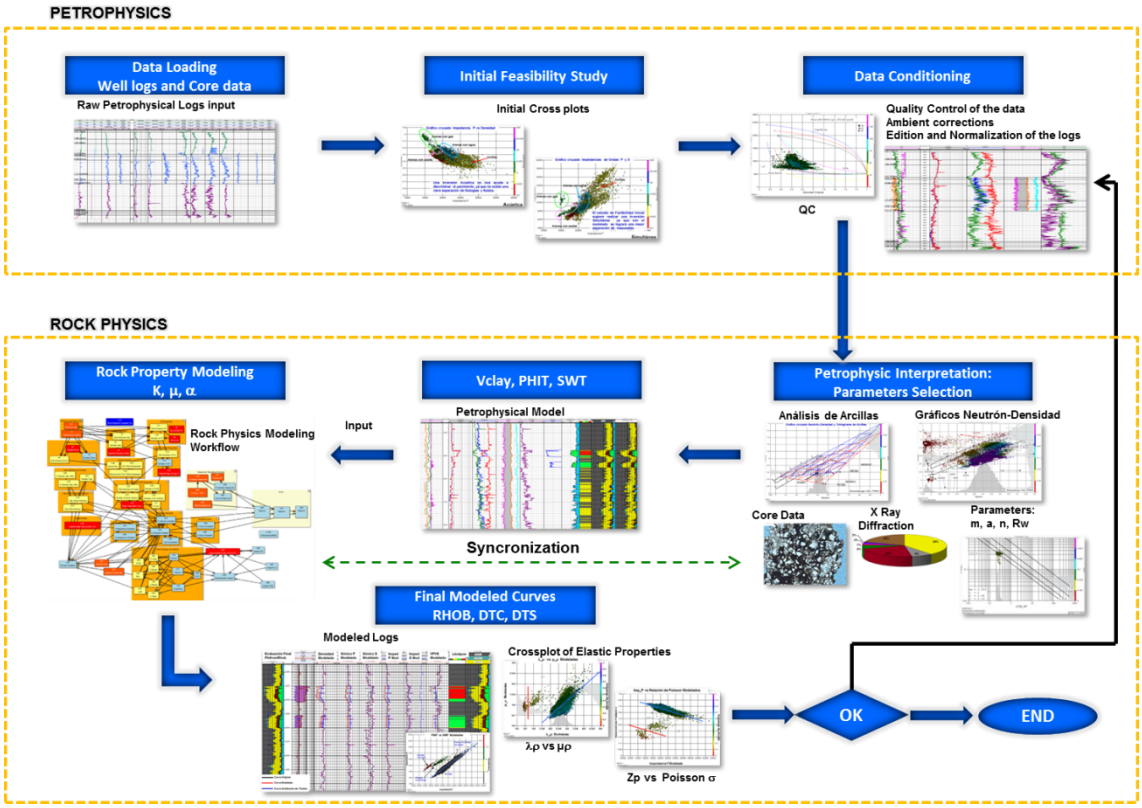

Figure 12-2 Basic Rock Fluid workflow is presented in the figure, this process is compsed of two main componentes, the petrophysics and afterwards he Rock physics phase.

12.7. Seismic Inversion Workflow

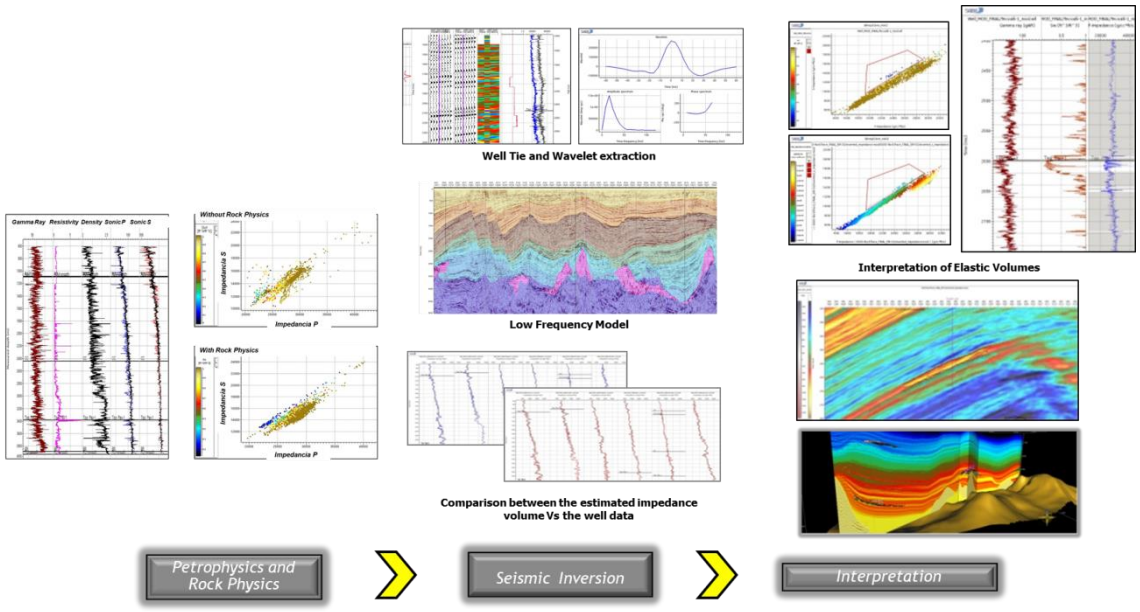

Figure 12-3 Seismic Inversion Workflow

12.8. AVO response

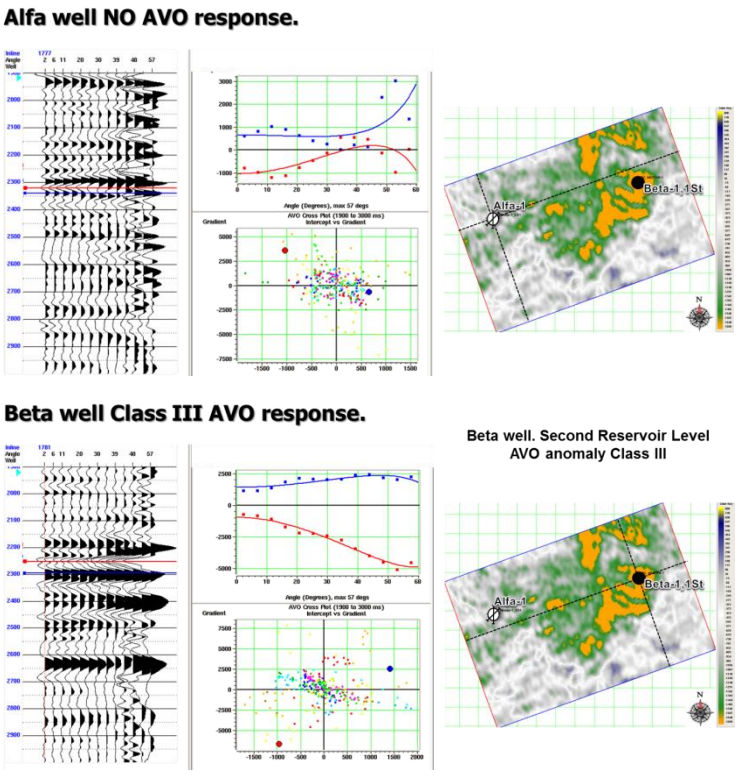

Figure 12-4 AVO response of the wells in the area. Alfa well no AVO anomalies, Beta Well Class III AVO .

Bibliography

Adeoti L., Onyekachi N., Olantinsu O., Fatoba J., Bello M., 2014., ¨Static Reservoir Modeling using well log and 3D Seismic data in the KN Field, Offshore Niger Delta, Nigeria¨ International Journal of Geosciences, 2014,5,93-106.

Aigner, T., Braun, S., Palermo, D., Blendinger, W., 2007., ¨3D geological modelling of a carbonate shoal complex: reservoir analogue study using outcrop data¨ First Break, Volume 25, August 2007.

Al-Bulushi, N., King, P.R., Blunt, M.J., Kraaijveld, M., 2010., “Generating a capillarity saturation – height function to predict hydrocarbon satrutration using artificial neural networks” Petroleum Geoscience, Vol. 16, 2010, pp. 77-85

Archie, G.E. (1942). "The electrical resistivity log as an aid in determining some reservoir characteristics". Petroleum Transactions of AIME 146: 54–62.

Asquith, G., and D. A. Krygowski (2004), Basic well log analysis, Second edition,
AAPG Methods in Exploration Series, No. 16, The American Association of Petroleum Geologists, Tulsa, ISBN: 0-89181-667-4.

Bahorich, M., Farmer M., 1992., “The coherence cube” The leading Edge (1995) 1053-1058.

Baker, O.R., Yarranton, W.H., Jensen, J.L., 2015., “Practical Reservoir Engineering and Characterization” Elsevier Editorial 2015.

Bulletin of the Mexican Association of Petroleum Geologist, Vol. XXV No. 1-3, January –March 1973

Cemen I., Fuchs J., Coffey B., Gertson R., Hager C., 2014” Correlating Porosity with Acoustic Impedance in Sandstone Gas Reservoirs: Examples from the Atokan Sandstones of the Arkoma Basin, Southeastern Oklahoma”., Search and Discovery Article #41255., February 2014.

Chopra S., Marfurt K.J, 2005., “Seismic Attributes- A historical perspective”., Geophysics, Vol. 70, No. 5 (September-October 2005);

Chopra, S., Marfurt, K.J., 2007., “Seismic Attributes for Prospect Identification and Reservoir Characterization” SEG Geophysical Development Series No. 11.

Connolly, P., 1999., “Elastic Impedance” The leading Edge, 18 (4), 438-452. 1999.

Contreras, A., Torres-Verdin, C., Kvien, K., Fasnacht, T., and Chesters, W., 2005., ”AVA stochastic inversion of pre-stack seismic inversion data and well logs for 3D reservoir modeling” 67th Annual Conference & Exhibition, EAGE, Paper T-015, 4 p.

Crain. E. R., 2016. “Crain's Petrophysical Handbook ONLINE version”. Available at: https://www.spec2000.net/00-resume.htm. [Accessed 1 June 2016].

Cuddy, S., Allinson, G. and Steele, R., 1993., “A simple, convincing model for calculating water saturations in Southern North Sea gas fields”, Paper H, SPWLA 34th Annual Logging Symposium, June 13th – 16th (1993).

Daly, C., Quental, S., Novak, D., 2010. “A Faster More Accurate Gaussian Simulation” AAPG Search and Discovery.

Dolberg D.M., Helgesen J., Hanssen T.H., Magnus I., Saigal G., 2000., “Porosity prediction from seismic inversion Levrans Field, Halten Terrace, Norway”., The leading Edge. April, 2000.

Dott, R.H. Jr & Bourgeois, J. 1982., “Hummocky cross stratification: significance of its variable bedding sequences”. Geological Society of America Bulletin, 93, 663–680.

Ellis V.D., Singer J.M., 2008., ¨Well Logging for Earth Scientist¨ Second Edition, Published by Springer

Fleming, B.W., 1995., “Tidal Signatures in Modern and Ancient Sediments”. Special Publication 24, Edited by Bartholoma, A., International Association of Sedimentologists. Blackwell Science, Oxford.

Goodway B., Chen T., Downton J., 1997., “Improved AVO Fluid Detection And Lithology Discrimination Using Lamé Petrophysical Parameters; “λρ”, μρ, λμ Fluid Stack”, From P And S Inversions.” Society of Exploration Geophysicist, 1997 SEG Annual Meeting, 2-7 November, Dallas, Texas.

Gray Goodway, B., Chen, T., Downton, J. 1997. Improved AVO fluid detection and lithology discrimination using Lame’s petrophysical parameters. Expanded Abstracts. CSEG, 1997 Convention.

Hampson, D., et al., 2001. Use of multiattribute transform to predict log properties from seismic data. Geophysics, Vol. 66, pp 230-236.

Harrison, B. and Jing, X.D., 2001, “Saturation Height Methods and Their Impact on Volumetric Hydrocarbon in Place Estimates”, Society of Petroleum Engineers, SPE.

Holdaway., K., 2014. “Harness Oil and Gas Big Data with Analytics: Optimize Exploration and Production with Data-Driven Models” Published by John Wiley & Sons. ISBN 9781118920894 (ePub).

Johnson, A., 1987., “Permeability averaged capillary data: a supplement to log analysis in field studies”, Paper EE, SPWLA 28th Annual Logging Symposium, June 29th – July 2nd (1987).

Latimer, B,R., Davison, R., Riel, P.V., 2000.," An interpreter's guide to understanding and working with seismic-derived acoustic impedance data.", The Leading Edge, 19, 242–256."

Leverett, M.C., 1941., "Capillary behaviour in porous solids" Petroleum Transactions of AIME 142 (1941) pp 152-169.

McCain W.D., 1990., "The properties of Petroleum Fluids, 2 Ed." Pennwell Puplishing Company.

Nanda C. N., 2016., "Seismic Data Interpretation and evaluation for Hydrocarbon Exploration and Production" Published by Springer International. ISBN 978-3-319-26491-2 (eBook).

Nichols G., 2009.,"Sedimenology and Stratigraphy"., Wiley-Blackwell., Second Edition.

Olea, R.A., 2012., "Geostatistics for Engineers and Earth Scientist." Springer Science, First edition December 2012.

Osman A.K., Yousef A.Z., Edrwards K., Hafez M., Sulistiono D., 2014.,"Geostatistical Inversion in Carbonate and Clastic Reservoirs: Oilfield Case Studies from Kuwait" Search and Discovery Article #20239 (2014) Posted March 19, 2014.

Padilla, R.J., 2014., "Tectonics of Eastern Mexico- Gulf of Mexico and its Hydrocarbon Potential" Search and Discovery Article #10622 August 2014.

Pettijohn F.J., Potter P.E., Raymond S., 2012.,"Sand and Sandstone" Second Edition Springer Science & Business Media.

Simm, R., Bacon, M., 2014., "Seismic Amplitude: An interpreters handbook" Cambridge University Press, First edition.

Skelt, C. and Harrison, R.: "An integrated approach to saturation height analysis", Paper NNN, SPWLA 36th Annual Logging Symposium, (1995).

Slatt R. M.,2013." Stratigraphic Reservoir Characterization for Petroleum Geologists, Geophysicist, and Engineers Origin, Recognition, Initiation and Reservoir Quality 2 Ed." Development in Petroleum Science Volume 61.

Tenente Pascoal, D.E., 2015., "Saturations Calculations Using Saturation Heigth Modeling on the well Mariana, offshore Lower Congo Basin" Master Thesis Norwegian University of Science and Technology, Department of Petroleum Engineering and Applied Geophysics.
Thigpen, B.B., Dalby, A.E., Landrum R., 1975., "Special Report on Subcommite on Polarity Standards" Geophysics, 40, no. 04, 694-699.

Timur, A. 1968., "An Investigation Of Permeability, Porosity, & Residual Water Saturation Relationships For Sandstone Reservoirs." The Log Analyst IX.

Wiltgen, N.A., Calvez, J.L. Owen K., 2003. "Methods Of Saturation Modelling Using Capillary Pressure Averaging and Pseudos." SPWLA 44th Annual Logging Symposium, 2003.

White, R.E., 1997., “The accuracy of well ties: practical procedures and examples, Expanded Abstract” 67th SEG Meeting, Dallas.

Yilmaz, O., Doherty, S.M., 1987. “Seismic Data Analysis, Processing, Inversion, and Interpretation of Seismic Data” First Edition, Society of Exploration Geophysicists.